Acta technologica agriculturae 3
Nitra, Slovaca Universitas Agriculturae Nitriae, 2011, s. 57–60

USE OF NEAR INFRARED SPECTROSCOPY WHIT FOURIER TRANSFORM TO ANALYSIS OF CURD CHEESE "OLOMOUCKÝCH TVARŮŽKŮ "

VYUŽITIE BLÍZKEJ INFRAČERVENEJ SPEKTROSKOPIE PRI ANALÝZE „OLOMOUCKÝCH TVARŮŽKŮ"

Monika KOZELKOVÁ, Květoslava ŠUSTOVÁ, Táňa LUŽOVÁ, Aneta BUBENÍČKOVÁ

Mendel University in Brno, Czech Republic

The aim of this study was to check the use of NIR technique for assessment of dry matter (DM), active acidity (pH), sodium chloride (NaCl) of curd cheese to name "Olomoucké tvarůžky" by FT-NIR. Seventy two samples were obtained directly from producer, and stored at 5 °C during five weeks. Spectra were measured in the reflectance mode with a compressive cell (radius 1 cm) wave number between (4 000 – 10 000) cm^{-1}, averaging 80 scans, spectral resolution 4 cm^{-1}. Correlations between reference values of chemical properties and NIR reflectance data were examined using the multivariate method of partial leas squares (PLS) regression. The correlation coefficient for DM was 0.952 and those for pH and NaCl were 0.905; 0.975 respectively. The standard error of the calibration for DM, pH and NaCl were found 0.285; 0.245; 0.090 respectively. The calibration models developed were verified by cross validation. The study show that FT-NIR spectroscopy can be used for determination of some chemical properties of curd cheese – "Olomoucké tvarůžky"

Key words: FT-NIR spectroscopy, curd cheese, calibration, "Olomoucké tvarůžky"

Near infrared spectroscopy is a physical method, which use the radiation of known wave number (usually 12 500 – 4 000 cm^{-1}) and gives a complete picture of the composition of the sample (Mlček, 2008). Principle of this method is the absorption or reflection of radiation passing through the sample, which involves changes in rotational vibrational energy of molecules in response to changes in dipole moment of the molecule. Analytical output is the infrared spectrum, which is a graphic display of the functional dependence of energy, usually expressed as a percentage of transmittance (T) or absorbance units (A) on the wavelength of incident radiation. FT-NIR is used widely for determination of organic constituents in feeds, foods, products and related materials (Sorensen and Jepsen, 1998). The technique is available for many applications, because it is non-destructive, rapid, cheap and multiparametric, is an alternative technique to the current methods used for qualitative and quantitative assessment of milk and dairy products (Coppa et al., 2010). The technique is also suitable for at-line and on-/in-line process control. Practical use of NIR spectroscopy in dairies has been mainly used to determine of dry matter, fat, protein, and lactose in raw and dry milk, yogurt, butter, hard and semi hard cheeses (Čurda and Kukačková, 2004). "Olomoucké tvarůžky" are sour curd smeared cheese, which are produced of industrial curd. However, little work has been done in curd cheese "Olomoucké tvarůžky" analyses, in literature reviewed only one article was found, which has been written by Dračková et al. (2009). These approaches can be combined with e.g. electrical and dielectrical properties of tested materials as described e.g. in Hlaváčová (2005).

Materials and methods

Samples

Seventy two samples were obtained directly from producer, and stored at 5 °C during five weeks and were analyzed for the calibration purposes. The samples were homogenized before the analysis. In the samples was assessed: dry matter content (DM), active acidity (pH), sodium chloride content (NaCl).

Reference Analysis

- Dry matter content (DM) – ČSN ISO 5534 2005: Cheese and processed cheese – Determination of total solids content (Reference method), Czech Standards Institute, Prague.
- pH – ČSN 570107 1980: Testing methods for natural and processed cheese. Determination of pH by potenciometry (Reference method), Czech Standards Institute, Prague.
- NaCl content – ČSN ISO 5943 1996: Cheese and processed cheese products. – Determination of chloride content. – Potentiometric titration method), Czech Standards Institute, Prague.

NIR analysis

NIR reflectance spectra were collected by the spectrophotometer Thermo NICOLET ANTARIS (Nicolet CZ s.r.o., Czech Republic). Spectra of samples were measured on the integration sphere in the reflectance mode with number 80 scans in wave number (10 000 – 4 000) cm^{-1} and spectral resolution 4 cm^{-1}. The samples were measured in compressive cell (radius 1 cm). Each sample was measured twice and average spectrum was used to create of calibration models.

Statistic

The calibration models for quantitative analysis were developed by using program TQ ANALYST (Nicolet CZ s.r.o, Czech Republic). The calibrations were performed the Partial least squares (PLS) algorithm using the first and second derivatives of the spectra. The important diagnostic instrument for PLS is the PRESS (Predicted Error Sum residual or squares), which allows us to estimate the optimal number of factors for calibration. PRESS value is the indicator of error PLS calibration method (Jankovská and Šustová, 2003). Reliability of the calibration model was validated by cross –

validation. The capability of the calibration models to predict the concentration of the components was expressed as correlation coefficient (R^2), standard error of calibration (SEC), calibration coefficient of variation (CCV), standard error of prediction (SEP), prediction coefficient of variation (PCV), xNIR – average of NIR values, x REF – average of reference values, standard error of difference (SD), linear regression line ($y = bx + a$). The range of reference values for each parameter was expressed as average (x_p), standard error average (x_s), minimum value (min), maximum value (max).

Result and discussion

The total of 72 curd cheese was used for the development of the calibration models. Samples were measured in the wave number between (10 000 – 4 000) cm^{-1}. Spectrum of the curd cheese – "Olomoucké tvarůžky" is presented in Figure 1. The ranges of the reference values for the monitored parameters (DM, pH, NaCl) were expressed by average and standard error of average (Table 1).

Table 1 Values of the individual parameters established by reference methods (n = 72)

Parameter (1)	min (5)	max (5)	x_p (6)	x_s (7)
DM in $g.kg^{-1}$ (2)	34.54	38.97	37.04	0.93
pH (3)	5.45	7.70	6.14	0.57
NaCl in $g.kg^{-1}$ (4)	4.93	6.56	5.57	0.40

DM – dry matter content, pH – active acidity, NaCl content, min, max – minimum and maximum values, x_p – average, x_s – standard error of average

Tabuľka 1 Hodnoty jednotlivých parametrov určené referenčnými metódami (n = 72)
(1) parameter, (2) obsah sušiny, (3) aktívna kyslosť, (4) obsah NaCl, (5) minimálna a maximálna hodnota, (6) x_p – priemer, (7) x_s – smerodajná odchýlka priemeru

Basic statistical parameters of the calibrated components are shown in Table 1. The TQ ANALYST was used to create the chemometric models. The calibration was created by using the partial leas square (PLS) method. With the help of diagnostic devices called Spectrum Outlier and Leverage were removed outlying standards, in which reference values were established incorrectly or there was a spectrum deviation. The exact number of samples used for calibration is shown in Table 2. In assessment of the dry matter, pH and NaCl was obtained a lower standard error of cross validation after the modification of the calibration model with using the first derivative. An important diagnostic tool is the dependence of PRESS (predicted residual error sum of squares) on the number of PLS factors used for calibration, which makes it possible to estimate the optimum number of factors (Dračková et al., 2006). The PRESS behavior is shown in Figure 2.

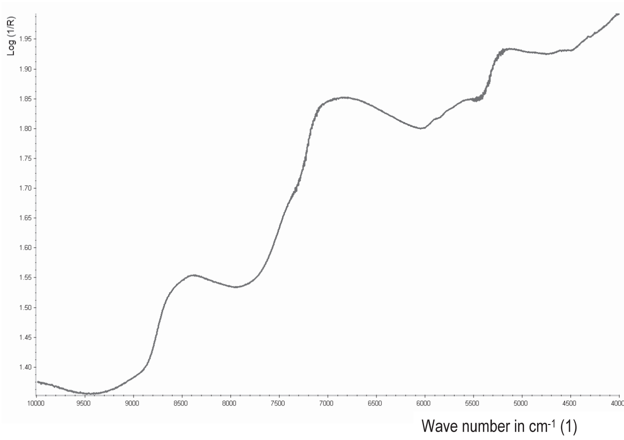

Figure 1 Near infrared spectrum of Curd cheese – "Olomoucké tvarůžky"
Obrázok 1 Infračervené spektrum "Olomoucké tvarůžky"
(1) vlnové číslo

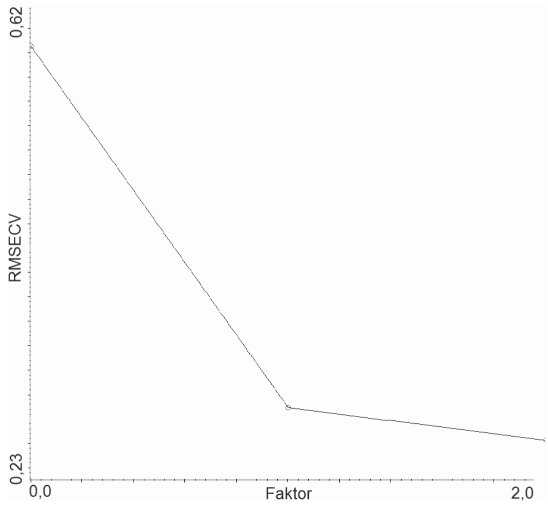

Figure 2 Predicted residual error square sum (PRESS) for NaCl
Obrázok 2 Diagnostický nástroj, predpokladaná chyba sumy štvorcov (PRESS) pre NaCl

The calibration models were verified by the cross-validation. The capability of the calibration models to predict the concentration of the components was expressed as standard error of calibration (SEC), standard error of prediction (SEP) and correlation coefficient (R^2) between reference and prediction values. The accuracy and the precision of the calibration was verified by calibration coefficient of variation

Table 2 Calibration results of the individual parameters established by FT-NIR spectroscopy (n = 72)

Parameter (1)	$y = bx \pm a$ (2)	SEC (3)	CCV in % (4)	R^2 (5)	Derivate (6)	PLS (7)
DM in $g.kg^{-1}$	$y = 0.9063x + 3.4695$	0.285	0.77	0.952	1	5
pH	$y = 0.8183x + 1.1149$	0.245	3.99	0.905	1	2
NaCl in $g.kg^{-1}$	$y = 0.9508x + 0.274$	0.090	1.62	0.975	1	5

$y = bx \pm a$ – linear regression line, SEC – standard error of calibration, CCV – calibration coefficient of variation, R^2 – correlation coefficient, PLS – number of PLS factors

Tabuľka 2 Kalibračné výsledky jednotlivých parametrov určených FT-NIR spektroskopiou (n = 72)
(1) parameter, (2) lineárna regresná krivka, (3) smerodajná odchýlka kalibrácie, (4) variačný koeficient kalibrácie, (5) koeficient korelácie, (6) derivácia, (7) počet PLS faktorov

Table 3 Validation results of the individual parameters established by FT-NIR spectroscopy (n = 72)

Parameter (1)	*y = bx ± a* (2)	SEP (3)	PCV in % (4)	R^2 (5)
DM in g.kg^{-1}	y = 0.539x + 17.119	0.572	1.54	0.801
pH	y = 0.7917x + 1.2772	0.263	4.48	0.889
NaCl in g.kg^{-1}	y = 0.4823x + 2.902	0.255	4.56	0.802

y = bx + a – linear regression line, SEP – standard error of prediction, PCV – prediction coefficient of variation, R^2 – correlation coefficient

Tabuľka 3 Validačné výsledky jednotlivých parametrov určených FT-NIR spektroskopiou (n = 72)
(1) parameter, (2) lineárna regresná krivka, (3) smerodajná odchýlka predikcie, (4) variačný koeficient predikcie, (5) koeficient korelácie

(CCV), prediction coefficient of variation (PCV), by the testing of the coefficients of the regression line between measured and predicted values and by Student test for comparison of the means of two related (paired) samples.

The output of the obtained calibration results is given in Table 2 and 3. The correlation coefficient R^2 shows the quality of regression dependence between measured values and predicted by NIR spectroscopy. The dependence of the correlation coefficient from 0.95 to 0.99 is considered as very strong, strong enough from 0.80 to 0.94 and from 0.50 to 0.79 points to moderate dependence (Dračková et al., 2009).

The correlation coefficients of calibration for measured quantities (DM and NaCl) are considered as very strong dependence (> 0.95), it means that the calibration models work well and the predicted values for the calibration symplex match to the value obtained by the reference method. The correlation coefficient of calibration for pH is considered as strong enough dependence. The best result was acquired for NaCl assessment, where R^2 = 0.975 and SEC = 0.090 g.kg^{-1} (Figure 3).

To develop of a validation model with using the cross-validation method, the same calibration´s samples was used. The correlation coefficients of validation for measured quantities (DM and NaCl) are considered strong enough dependence. The best result was acquired for NaCl assessment, where R = 0.802 and SEP = 0.255 g.kg^{-1}. Another criterion for assessing of the success of the calibration is coefficient of variation (CCV) and prediction coefficient of variation (PCV). Dependable calibration takes place in the case of the value of the calibration coefficient of variation CCV being lower than 5 %, and the value of the prediction coefficient of variation being lower than 10 % (Jankovská and Šustová, 2003). Based on obtained values CCV and PCV, we can state that calibration models were reliably created for all the monitored parameters.

Table 4 shows the results of statistical analysis of the NIR predicted values and reference values which were tested using Student t-test. The aim of the t-test is to determine, whether the values of the two methods (NIR, reference) are not significantly different.

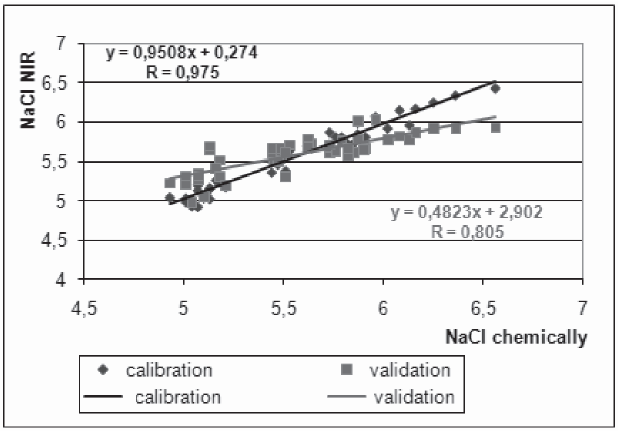

Figure 3 Calibration and validation model for NaCl content
Obrázok 3 Kalibračný a validačný model pre obsah NaCl

If is t_{stat} lower than $t1_{krit}$ and $t2_{krit}$, calibration model will be functional and values will be not significantly different from each other. It follows from Student t-test, that there not significant difference between NIR estimate and the result of reference method (Table 4).

The work, which was engaged examining curd cheese – "Olomoucké tvarůžky" using NIR spectroscopy has been published by Dračková et al. (2009). The work was named Determination of polyamine content in curd cheese by Near-infrared reflectance spectrometry. Sultaneh and Rohm (2007) were dealt with providing a dry matter and protein of curd cheese. Based on approximately 250 curd samples, they built calibration models with using partial least squares regression. The calibration models resulted in coefficients of determination of R^2 = 0.994 for dry matter and R^2 = 0.985 for protein content for unhomogenized curd, which improved only slightly after subjecting the curd to homogenization.

Conclusion

The results proved the possibility of determining the selected qualitative parameters (dry matter, pH and NaCl) by using of NIR spectroscopy in the case of curd cheese – „Olomoucké tvarůžky". Relatively high correlation coefficients for calibration were attained in almost all models. The best result was acquired for NaCl assessment, where R^2 = 0.975 and SEP = 0.090 g.kg^{-1}. Statistical verification by using of indicators the reliability of the calibration model (CCV and PCV) was right. Statistical verification by means of the Student T-test did not show any statistically conclusive differences between the reference and the predicted NIR values in any cases. As confirmed by results obtained from calibration and validation, near infrared spectroscopy is a potential and powerful method for the rapid monitoring of some chemical parameters of curd cheese – "Olomoucké tvarůžky".

Table 4 Statistical values for curd cheese – "Olomoucké tvarůžky" obtained by Student t-test

Parameter (1)	xNIR (2)	xREF (3)	SD (4)	t_{stat}	$t1_{krit}$ (5)	$t2_{krit}$ (6)
DM in g.kg^{-1}	37.04	37.04	0.137	0.000	1.679	2.014
pH	6.14	6.14	0.073	0.021	1.653	1.973
NaCl (g.kg^{-1}	5.57	5.57	0.059	0.032	1.679	2.013

xNIR – average of NIR values, xREF – average of reference values, SD – standard error of difference, $t1_{krit}$ – table value for α = 0.05, $t2_{krit}$ – table value for α = 0.01

Tabuľka 4 Štatistické hodnoty pre Olomoucké tvarůžky získané Studentovým t-testom
(1) parameter, (2) priemer NIR hodnôt, (3) priemer referenčných hodnôt, (4) smerodajná odchýlka rozdielu, (5) tabuľková hodnota pre úroveň α = 0,05, (6) tabuľková hodnota pre úroveň α = 0,01

Súhrn

Cieľom práce bolo zistiť, či je možné použiť FT-NIR spektroskopiu na stanovenie niektorých chemických parametrov: obsah sušiny (DM), aktívna kyslosť (pH), obsah chloridu sodného (NaCl) v tvarohovom syre s názvom "Olomoucké tvarůžky". Sedemdesiatdva vzoriek sa získalo priamo od výrobcu a skladovali sa pri teplote 5 °C počas piatich týždňov. Spektrá boli merané v režime reflektancie s využitím kompresnej kyvety (polomer 1 cm) v rozsahu (4 000 – 10 000) cm^{-1}, s priemerom 80 skanov a pri spektrálnom rozlíšení 4 cm^{-1}. Vzťah medzi referenčnými hodnotami chemických vlastností a NIR hodnotami bol skúmaný multivariačnou metódou čiastočných najmenších štvorcov (PLS – partial least squares). Korelačný koeficient pre DM bol 0,952 a pre pH a NaCl 0,905; 0,975. Ďalej sa zistila smerodajná odchýlka kalibrácie pre DM, pH a NaCl: 0,285; 0,245; 0,090. Vytvorené kalibračné modely boli overené pomocou krížovej validácie. Štúdia ukazuje, že FT-NIR spektroskopia môže byť použitá na stanovenie niektorých chemických vlastností tvarohového syra – "Olomoucké tvarůžky".

Kľúčové slová: FT-NIR spektroskopia, tvaroh, kalibrácia, "Olomoucké tvarůžky"

Acknowledgement

This research has been supported by the project No. TP 10/2010 "Technological and microbial parameters of raw material and their influence on quality of sour curd smeared cheese" which is financed by the Internal Grant Agency of Mendel University in Brno and by the Research plan the Ministry of Education, Youth and Sports of the Czech Republic 2B08069 National plan of research – NPV II, plan 2B – Healthy and quality of life.

References

COPPA, M. – FERLAY, A. – LEROUX, CH. – JESTIN, M. – CHILIARD, Y. – MARTIN, B. – ANDUEZA, D. 2009. Prediction of milk fatty acid composition by Near-infrared reflectance spectroscopy. In: International Dairy Journal, 2010, no. 20, p. 182 – 189

ČURDA, L. – KUKAČKOVÁ, O. 2004. NIR spektroskopy: a useful tool for rapid monitoring of processed cheeses manufacture. In: Journal of Food Engineering, 2004, no. 61, p. 557 – 560

ČURDA, L. – KUKAČKOVÁ, O. – NOVOTNÁ, M. 2002. Near-infrared spectroscopy and its application to milk and dairy products analysis. In: Chem Listy, vol. 96, 2002, p. 305 – 310

DRAČKOVÁ, M. – JANDOVÁ, T. – STANDAROVÁ, E. – KORDIOVSKÁ, P. – BORKOVCOVÁ, I. – JANŠTOVÁ, B. – NAVRÁTILOVÁ, P. – VORLOVÁ, L. 2009. Stanovení obsahu polyaminů v tvarůžcích pomocí blízké infračervené reflektanční spektrometrie. In: Acta fytotechnica et zootechnica, 2009, p. 121 – 126

DRAČKOVÁ, M. – HARDA, L. – TATRANOVÁ, I. – VOZKOVÁ, L. – VORLOVÁ, L. 2006. Využití FT-NIR v analýze pasterovaného mléka. Mléko a sýry, 2006, s. 158 – 161

HLAVÁČOVÁ, Z. 2005. Utilization of electrical properties of granular and powdery materials. In: International Agrophysics, vol. 19, 2005, p. 209 – 213

JANKOVSKÁ, R. – ŠUSTOVÁ, K. 2003. Analysis of cow milk by near-infrared spectroscopy. In: Czech Journal of Food Science, 2003, no. 4, p. 123 – 128

MLČEK, J. 2008. Využití NIR spektrometrie pro hodnocení kvality potravin a potravinových surovin, Disertační práce. Brno : Mendelova univerzita, 2008, s. 12 – 18

SORENSEN, L. K. – JEPSEN, N. 1998. Assessment of sensory properties of cheese by Near-infrared Spectroscopy. In: Dairy Journal, 1998, no. 8, p. 863 – 861

SULTANEH, A. – ROHM, H. 2007. Using near-infrared spectroscopy for the determination of total solids and protein content in cheese curd. In: International Journal of Dairy Technology, vol. 60, 2007, no. 4, p. 241 – 244

Contact address:
Ing. Monika Kozelková, Technologie potravin, Mendlova univerzita v Brně, Zemědělská 1, 613 00 Brno, Česká republika, e-mail: xkozelk2@mendelu.cz, ✆ 777 876 104

Acta technologica agriculturae 3
Nitra, Slovaca Universitas Agriculturae Nitriae, 2011, s. 61–66

EVALUATION OF SELECTED AGRO-PHYSICAL PROPERTIES OF A ROOT VEGETABLE

ZHODNOTENIE VYBRANÝCH AGROFYZIKÁLNYCH VLASTNOSTÍ KOREŇOVEJ ZELENINY

Ján JOBBÁGY, Dalibor GABAJ, Július ÁRVAY

Slovak University of Agriculture in Nitra, Slovak Republic

This paper deals with evaluating the variability of selected agro-physical properties of carrots. The variety grown was the carrot Tinga. The average value of yield for the whole field was 10.63 $t.ha^{-1}$. The yield values in individual monitoring points ranged from 9.03 $t.ha^{-1}$ (monitoring point 6) to 13.09 $t.ha^{-1}$ (monitoring point 3). The field was irrigated using the Bauer Rainstar T41 reel hose irrigation machine. The average value of a coefficient of slenderness within the field under investigation achieved 4.65; the values ranged from 4.36 (monitoring point 2) to 4.92 (monitoring point 1). The average value of a coefficient of convergence was 5.62; the values of this coefficient were in the interval from 5.1 (monitoring point 2) to 6.2 (monitoring point 3).

Key words: carrots, agro-physical properties, conicity of carrots, coefficient of slenderness and coefficient of convergence of carrots

Transition to the third millennium was accompanied by a transition from Green Revolution, when environmental issues were accentuated, to the Blue Revolution characterised by combating water and a struggle for water. In regions lacking natural water resources, this means the struggle for water, food and for survival (Hríbik, 2006).

Currently, the main objective is the cost reduction in producing agricultural products and the reinforcement of the overall competitiveness in the global market with agricultural commodities. This trend is known as precision agriculture (Nozdrovický, 1999).

New methods in the field of rational intensification of crop production, focusing on plant nutrition by connecting irrigation with fertilisation, are providing extensive opportunities for the control and optimisation of nutritional and water regime during the growing season. Despite the knowledge already obtained, it is necessary to elaborate and better characterise the conditions intensifying production and increasing the availability of water and nutrients from fertilisers by crops grown in different soil and climatic conditions, and at a constant need to further protect the environment and health condition of production and the consumer (Nielsen and Roberts, 1996; Paoli, 1997).

The objective of this paper is to evaluate the variability of agro-physical properties of the root vegetable in selected monitoring points of the investigated field.

Materials and methods

The Paulen farm was founded in 1996. It is located in West Slovakia, in the district of Topoľčany, and currently manages 220 ha of agricultural land. Its business interests extend to a wider area of Topoľčany. Carrots were grown in a field with the total area of 1.85 ha (Figure 1). The results of a soil analysis have shown that the soil is slightly acid (Table 1). Crop yields as well as carrots are significantly influenced by rainfall; the results are shown in Table 2. The company is monitoring the rainfall amount using a rain gauge.

The crop was irrigated using the Bauer Rainstar T41 reel hose irrigation machine (Figure 1). The water demand of

Table 1 Content of nutrients and soil pH

Sample (1)	pH	P in $mg.kg^{-1}$	K in $mg.kg^{-1}$	Mg in $mg.kg^{-1}$
1	6.3	31	234	405
2	6.7	33	222	336
Average (2)	6.5	32	228	370
Evaluation (3)	slightly acid (4)	low (5)	medium (6)	high (7)

Tabuľka 1 Zásoba živín a pH
(1) vzorka, (2) priemer, (3) zhodnotenie, (4) slabo kyslá, (5) nízka, (6) stredná, (7) vysoká

Table 2 Rainfall in the investigated field

Months (1)	1	2	3	4	5	6	7	8	9	10	11	12	Per year (2)
2009	41	28	46	7	85	50	67	6	9	62	61	53	515
2010	35	30	16	74	138	121	78	94	88	–	–	–	–

Tabuľka 2 Zrážky na zameranom pozemku
(1) mesiace, (2) za rok

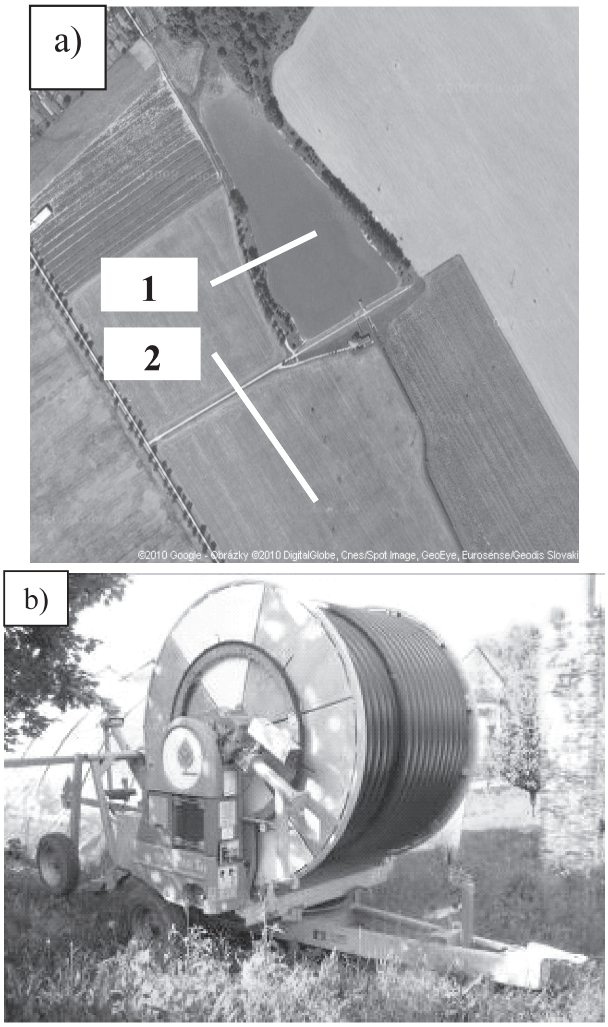

Figure 1 a – Position of the investigated field, b – reel hose irrigation machine
1 – water resource, 2 – investigated field
Obrázok 1 a – zameraný pozemok, b – pásový zavlažovač
1 – zdroj vody, 2 – pozemok

carrots is 520 – 620 mm per growing season. In our conditions, its successful growing during an average year requires to replenish natural rainfall with irrigation water ranging from 120 mm to 180 mm. The field boundaries were determined using a hand-held GPS receiver – Leica GS20. After setting up the necessary functions of the device, it is necessary to go around the field boundaries and to save the data gathered. The layout of monitoring points for taking samples was determined by means of a computer.

Figure 2 Field boundaries and monitoring points
Obrázok 2 Zameraný pozemok a monitorovacie body

The agro-physical properties were determined in 6 monitoring points. We focused on the following parameters of carrot roots:

- length (mm),
- conicity ($mm.mm^{-1}$) derived from the upper and lower carrot diameter,
- yield ($t.ha^{-1}$).

Conicity:

$$Ku = \frac{\phi_h - \phi_k}{\ell}$$

where:

ϕ_h – diameter at the root head (m)
ϕ_k – diameter at the root end (m)
ℓ – root length (m)

The coefficient of convergence (λ_1) is expressed by the ratio between the diameters in the upper (ϕ_h) and lower (ϕ_k) parts of the root. The coefficient of slenderness (λ) is given by the ratio between the length (ℓ) and the upper diameter (ϕ_h) of the root. The samples were taken from the length of 1.33 m (in one row), corresponding to an area of 1 m^2. The following parameters were determined:

- weight of all of the samples taken from 1 m^2 (kg),
- weight of individual roots (kg),
- length of individual roots (m),
- diameters of the upper and lower parts of roots (m).

Results and discussion

Monitoring point 1

Table 3 shows the results of measured parameters in monitoring point 1 (descriptive statistics). The total weight of the sample taken was 1 061 g; there were 22 pieces of carrots. The minimum root weight was 12 g, and the values reached up

Table 3 Descriptive statistics of measured parameters, monitoring point 1

Parameter (1)	Length in mm (2)	Weight in g (3)	Conicity (4)
Mean (5)	110.36	48.23	0.171
Standard deviation (6)	34.61	34.83	0.045
Minimum (7)	53	12	0.078
Maximum (8)	170	140	0.262
Number of samples (9)	22	22	22
Coefficient of variation (10)	31.36	72.23	26.25

Tabulka 3 Popisná štatistika nameraných parametrov, monitorovací bod 1
(1) parameter, (2) dĺžka, (3) hmotnosť, (4) kužeľovitosť, (5) priemer, (6) smerodajná odchýlka, (7) minimum, (8) maximum, (9) počet, (10) variačný koeficient

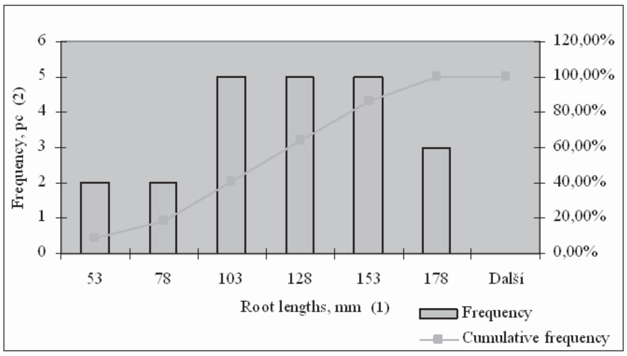

Figure 3 Length of roots, monitoring point 1
Obrázok 3 Dĺžka koreňov, monitorovací bod 1
(1) dĺžka koreňov, (2) početnosť

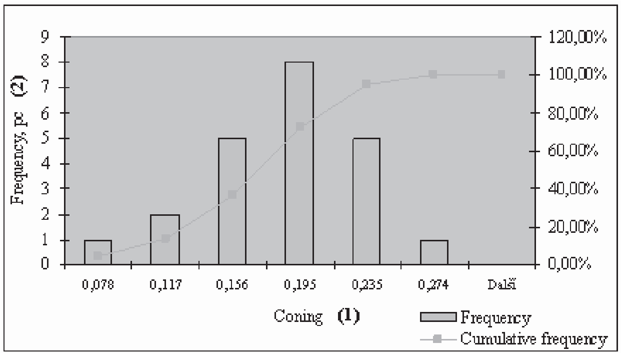

Figure 5 Conicity, monitoring point 1
Obrázok 5 Kužeľovitosť, monitorovací bod 1
(1) kužeľovitosť, (2) početnosť

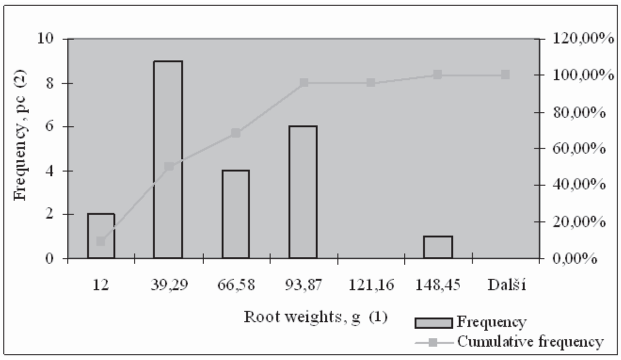

Figure 4 Weight of roots, monitoring point 1
Obrázok 4 Hmotnosť koreňov, monitorovací bod 1
(1) hmotnosť koreňov, (2) početnosť

to 140 g. The average value was 48.23 g, with a high coefficient of variation (72.23 %). The samples of carrots were separated from foliage and weighted after that. The results show that the average yield of carrots in monitoring point 1 was 10.61 $t.ha^{-1}$. Biological yield belongs to the most important production indicators. The length values in monitoring point 1 ranged from 53 mm to 170 mm. The value of the coefficient of variation for the length was only 31.36 %. The average length of roots depends not only on the variety, but also on the soil penetration resistance, soil structure, intake of nutrients during the growing season, growing location, and the method of irrigation. The average conicity represented 0.171.

The graphic representation of frequency distribution results for the length of carrot roots is shown in Figure 3. The frequency distribution for the net weight is shown in Figure 4, and Figure 5 is for conicity. Carrots need nutrients, water, light, and space sufficient for their continuous development.

Other monitoring points

In monitoring point 2, there was an increase in the total weight of roots from the sample taken in relation to monitoring point 1. The resulting value was 1309 g. This change also indicates an increase in the hectare yield of up to 13.09 $t.ha^{-1}$. There were 26

Table 4 Descriptive statistics of measured parameters, other monitoring points

Parameter (1)	Monitoring point (2)	Mean (3)	Standard deviation (4)	Minimum (5)	Maximum (6)	Number of samples (7)	Coefficient of variation (8)
Length in mm (9)	2	108.54	42.27	53	168	26	38.95
	3	113.09	44.85	53	168	22	39.66
	4	107.19	41.04	53	173	21	38.29
	5	107.25	38.47	53	166	20	35.87
	6	98.77	35.23	53	167	22	35.67
Weight in g (10)	2	50.35	38.49	12	148	26	76.46
	3	57.32	37.24	13	122	22	64.97
	4	51.24	37.66	15	150	21	73.50
	5	50.1	35.51	12	119	20	70.88
	6	41.05	32.97	12	138	22	80.32
Conicity (11)	2	0.171	0.051	0.069	0.277	26	29.82
	3	0.2	0.048	0.11	0.293	22	23.91
	4	0.189	0.059	0.081	0.298	21	31.22
	5	0.19	0.049	0.087	0.29	20	25.79
	6	0.186	0.046	0.097	0.278	22	24.73

Tabulka 4 Popisná štatistika nameraných parametrov, ostatné monitorovacie body
(1) parameter, (2) monitorovací bod, (3) stredná hodnota, (4) smer. odchýlka, (5) minimum, (6) maximum, (7) počet, (8) variačný koeficient, (9) dĺžka, (10) hmotnosť, (11) kužeľovitosť

carrots taken in the sample. The summary of descriptive statistics for monitoring point 3 is shown in Table 4. The total weight of the sample taken was 1 261 g. This means that the average yield of carrots in monitoring point 3 was 12.61 $t.ha^{-1}$ (number of carrots: 22). The total weight of the sample taken in monitoring point 4 was 1 076 g. In this point, 21 pieces of carrots were taken, and the yield was 10.76 $t.ha^{-1}$. The summary of descriptive statistics for monitoring point 5 is shown in Table 4. The average length was 107.25 mm. There were 20 pieces taken in this sample. The weight of carrot roots ranged from 12 g to 119 g; the average value being at 50.1 g. The yield achieved the value of 10.02 $t.ha^{-1}$.

Table 4 contains the results of descriptive statistics for the parameters (length, weight and conicity) in monitoring point 6. In this point, there were 22 pieces of carrots taken, having the weight of 903 g. The results show that the average yield of carrots in this point is the lowest of all monitoring points, equal to 9.03 $t.ha^{-1}$.

It results from the measured values of crop characteristics that the average biological yield varies depending on varieties, locations where the crop is grown and soil conditions. Crop characteristics indicate that the biological yield in our growing conditions is good. In year 2000, the average biological yield of the carrots Cartago in Kováčovce was 29.6 $t.ha^{-1}$ (min. 24.6 $t.ha^{-1}$ and max. 41.8 $t.ha^{-1}$); in the Bušince farm fields, the average biological yield in 2001 was 43 $t.ha^{-1}$ (min. 38 $t.ha^{-1}$ and max. 55 $t.ha^{-1}$). In the SELEKT Bučany farm fields (2001), the soil was prepared after ploughing only by ridging (in autumn), and before sowing during spring, the shape of mounds was renewed by ridging. The average biological yield of carrots was 64.8 $t.ha^{-1}$ (min. 38 $t.ha^{-1}$ and max. 82 $t.ha^{-1}$) (Poničan et al., 2004).

Coefficient of slenderness and coefficient of convergence

The coefficient of slenderness (λ) and coefficient of convergence (λ_1) were also evaluated. The coefficient of slenderness (λ) expresses the ratio between the average length of roots (ℓ) and the root head diameter (ϕ_h). A higher value of this coefficient means a slenderer root shape, and vice versa. The average value for all monitoring points was 4.65. The slenderest carrots were taken in monitoring point 1.

The coefficient of convergence (λ_1) expresses the ratio between the diameter at the root head (ϕ_h) and the diameter at the root end (ϕ_k). A value close to one represents a cylindrical root shape, and values greater than one mean conical root shapes. The average value obtained from 6 monitoring points was 5.62.

The values of convergence indicate that the roots of carrots were of the conical shape. The highest value was observed in roots occurring in monitoring point 3.

The slenderest root shape was observed in carrots grown in the Bušince farm fields in 2001 (Sugarsnax variety). The roots of this variety were characterised by the coefficient of slenderness of 8.67. The least slender shape was observed in carrots (Bolero variety) grown in Bučany (year 2001), where the value of slenderness was λ = 5.03 (Poničan et al., 2004). In terms of the root shape (cylindrical), the Bolero variety grown in Bučany (year 2001) comes closest to this value (the value for the root shape was λ = 1.25) (Poničan et al., 2004).

As regards the evaluation of agro-physical properties defined by the slenderness and convergence of roots, these properties are affected primarily by the characteristics of varieties and the way how the soil is prepared before sowing (Poničan et al., 2004). Achieving a high production in our climatic conditions requires irrigation.

A correct and adequate connection between both of the intensification factors, irrigation and fertilisation, enables to achieve high and economically interesting yields of a standard quality and good storage with regard to environmental protection (Pavelková, 2005).

The size of soil aggregates, soil compaction and an inappropriate structure can restrict plant emergence and deform roots. Carrot roots are unevenly developed, rough, deformed, with incisions at the top of the head of a green colour. On the other hand, the growing of carrots in profiled beds created by rotary cultivators provides nearly ideal conditions for the emergence, growth and development of plants (Poničan et al., 1998).

The technological procedure for soil preparation before sowing root vegetables significantly affects the physical and mechanical properties of the soil and consequently the quality of root vegetables (Poničan et al., 2004).

Other measurements under irrigation were carried out in Marcelová. The variety grown was the carrot Maestro. There were 73 pieces of carrots taken from the sample. To determine the hectare yield it was necessary to calculate the total value of the net weight of roots taken from the sample. The weight of roots ranged from 12.10 g to 269.8 g. The value of the coefficient of variation was 57.66 %, with the average value of 98.35 g. Also the yield of 71.79 t. ha^{-1} is a result of measuring the weight of roots. The comparison of yields enabled to reveal that the value obtained under fertilisation was higher by 2.32 $t.ha^{-1}$ (Jobbágy and Simoník, 2009).

When measuring the length of roots, the average value was 183.93 mm, with the coefficient of variation of 19.88 %. The length of roots ranged from 96 mm to 266 mm. When comparing these values with the values obtained under fertilisation, it is possible to find that the mean root length was higher at the lower value of the coefficient of variation. The mean value of conicity was 0.071, with the coefficient of variation of 32.82 %. The conicity ranged from 0.010 to 0.133 (Jobbágy and Simoník, 2009).

Slovakia produces 300 to 500 thousand tonnes of vegetables per year depending on the weather impact during a year. In years 2000 to 2004, the highest production of vegetables was achieved in year 2000 amounting to 469 thousand tonnes, and the lowest in year 2002 when 363 thousand tonnes of vegetables were produced. The share of individual groups of vegetables in the total production and total area in individual years does not change significantly. The harvested areas of carrots from years 2000 to 2004 range from 2 915 ha to 3 983 ha, with the largest area in year 2000 (3 983 ha). Production ranges from 37 079 t to 51 240 t. The highest production of carrots was achieved in year 2001 (51 240 t). The average yields of carrots for the period are fairly balanced and range from 11.89 $t.ha^{-1}$ to 13.89 $t.ha^{-1}$. The highest average yield for the whole of Slovakia was reached in year 2002 (13.89 $t.ha^{-1}$). The highest yields of carrot were recorded in the region of Trnava (20.42 $t.ha^{-1}$), followed by the regions of Nitra (16.57 $t.ha^{-1}$), Bratislava (15.39 $t.ha^{-1}$), Banská Bystrica (14.92 $t.ha^{-1}$), and Žilina (12.39 $t.ha^{-1}$). Relatively low yields were achieved in the regions of Košice (9.90 $t.ha^{-1}$) and Trenčín (8.28 $t.ha^{-1}$). The lowest average yield was achieved in the region of Prešov (7.06 $t.ha^{-1}$) (Valšíková and Robin, 2006).

Table 5 Slenderness and convergence of roots, carrot yield

Monitoring point (1)	Measured values in mm (2)		Coefficient of slenderness (λ) (3)	Coefficient of convergence (λ_1) (4)	Yield in t.ha^{-1} (5)
1	average root length (6)	110.36	4.92	5.6	10.06
	root head diameter (7)	22.41			
	root end diameter (8)	4.00			
2	average root length (6)	108.54	4.9	5.1	13.09
	root head diameter (7)	22.15			
	root end diameter (8)	4.31			
3	average root length (6)	113.09	4.36	6.2	12.61
	root head diameter (7)	25.91			
	root end diameter (8)	4.18			
4	average root length (6)	107.19	4.6	5.4	10.76
	root head diameter (7)	23.29			
	root end diameter (8)	4.29			
5	average root length (6)	107.25	4.56	5.9	10.02
	root head diameter (7)	23.5			
	root end diameter (8)	3.95			
6	average root length (6)	98.77	4.56	5.5	9.03
	root head diameter (7)	21.68			
	root end diameter (8)	3.9			
Average (9)			4.65	5.62	10.93

Tabuľka 5 Prepočítané hodnoty štíhlosti a zbiehavosti koreňov, úroda mrkvy
(1) miesto merania, (2) namerané hodnoty, (3) koeficient štíhlosti, (4) koeficient zbiehavosti, (5) úroda, (6) priemerná dĺžka koreňov, (7) priemer hlavy koreňov, (8) priemer konca koreňov, (9) priemer

Conclusions

When carrots are grown in beddings, costs will rise in relation to the conventional method. However, the achieved effect of yields is sufficiently significant, and the grower should take account of this production method. The current exercise price and the amount of production per hectare are decisive for economic benefits.

When the carrot shape is uneven, the selling price is reduced. Therefore, it is necessary that the soil be prepared by rotary cultivators and using the bedding method. It creates good conditions for a regular cylindrical shape of roots, and the highest hectare yields are reached under observed irrigation scheme and sufficient nutrients during the growing season.

Súhrn

V danom príspevku sa zaoberalo zhodnotením variability vybraných agrofyzikálnych vlastností porastu mrkvy. Pestovanou odrodou bola mrkva Tinga. Priemerná hodnota úrody na celom pozemku bola 10,63 t.ha^{-1}. Hodnoty úrod v jednotlivých monitorovacích bodoch boli od 9,03 t.ha^{-1} (monitorovací bod 6) do 13,09 t.ha^{-1} (monitorovací bod 3). Závlaha na pozemku sa uskutočnila pásovým zavlažovačom Bauer Rainstar T41. Priemerná hodnota koeficientu štíhlosti na zameranom pozemku bola 4,65. Hodnoty sa pohybovali v rozpätí od 4,36 (monitorovací bod 2) do 4,92 (monitorovací bod 1). Priemerná hodnota koeficientu zbiehavosti bola 5,62. Hodnoty koeficientu zbiehavosti boli od 5,1 (monitorovací bod 2) do 6,2 (monitorovací bod 3).

Kľúčové slová: mrkva, agrofyzikálne vlastnosti, kužeľovitosť mrkvy, koeficient štíhlosti a zbiehavosti

This paper is related to research project VEGA No 1/0407/11 "Research of the effectiveness of growing arable crops with the support of spatially variable irrigation" conducted at the Department of Machines and Production Systems, Faculty of Engineering, Slovak University of Agriculture in Nitra.

References

HRÍBIK, J. 2006. Úsporné závlahové technológie z aspektu ochrany vodných zdrojov. Príspevok do zborníka, Medzinárodné sympózium VODA PRE ŽIVOT – VODA ŽIVEL, v rámci 23. ročníka medzinárodného filmového festivalu AGROFILM 2006 v Nitre, s. 82 – 91. ISBN 80-89162-23-1. Available at: http://www.fem.uniag.sk /acta/sk/2/acta _horticulturae_et_regiotecturae/obsah/2003/1/48/

JOBBÁGY, J. – SIMONÍK, J. 2009. Vplyv prihnojovacej techniky na vybrané agrofyzikálne vlastnosti koreňovej zeleniny. In: Acta technologica agriculturae, roč. 12, 2009, č. 3, s. 80 – 85. ISSN 1335-2555.

NIELSEN, D. – ROBERTS, T. L. 1996. Potassium fertigation of high density apple orchards. In: Better Crops with Plant Food, vol. 80, 1996, no. 4, p. 12. ISSN 0006-0089

NOZDROVICKÝ, L. 1999. Cielené (presné) poľnohospodárstvo ako nová etapa technizácie a intelektualizácie poľnohospodárstva. In: Vytváření ziskového zemědělství. Precizní zemědělství: Sborník referátů z konference – I. Praha: TOKO A/S a.s., 1999, s. 101 – 114. ISBN 80-902411-5-X.

PAOLI, N. 1997. What does fertigation have to offer? Obstbau-Weinbau, vol. 34, 1997, no. 1, p. 10 – 13

PAVELKOVÁ, A. 2005. Vplyv hnojenia a zavlažovania na senzorickú kvalitu jabĺk. In: Autoreferát dizertačnej práce. Nitra : SPU, 2005, 19 s. Available at: http://www.uniag.sk/SKOLA/rvv/doc/ddiz/2005/ adriana_pavelkova.pdf

PONIČAN, J. – JECH, J. – ANGELOVIČ, M. 1998. Vplyv spracovania pôdy na jej vlastnosti. In: Technika a technológie pre udržateľné poľnohospodárstvo: Zborník referátov z medzinárodnej vedeckej konferencie : Nitra 4. 6. 1998. Nitra : SPU, 1998, s. 58–64. ISBN 80-7137-495-4.

PONIČAN, J. – JECH, J. – ANGELOVIČ, M. – ŽITŇÁK, M. 2004. Vplyv vlastností pôdy na agrofyzikálne vlastnosti koreňovej zeleniny. In: Acta technologica agriculturae, roč. 7, 2004, č. 4, s. 94 – 98. ISSN 1335-2555.

VALŠÍKOVÁ, M. – ČERVENKA, J. 2006. Produkcia koreňovej zeleniny v SR. [online]. Výskumný ústav zeleninársky, 2006. [cit. 4.4.2011Available at: <http://www.agroporadenstvo.sk/rv/zelenina/prod_koren_zel.htm?start>

Contact address:
Ing. Ján Jobbágy, PhD., Department of Machines and Production Systems, Slovak University of Agriculture in Nitra, Tr. A. Hlinku 2, 949 76 Nitra, e-mail: Jan.Jobbagy@uniag.sk

Acta technologica agriculturae 3
Nitra, Slovaca Universitas Agriculturae Nitriae, 2011, s. 66–68

ASSESSMENT OF WALL STRUCTURES IN TERMS OF TEMPERATURE DAMPING

POSÚDENIE STENOVEJ KONŠTRUKCIE Z HĽADISKA TEPLOTNÉHO ÚTLMU

Štefan POGRAN, Tímea REICHSTÄDTEROVÁ, Dušan PÁLEŠ, Jana LENDELOVÁ

Slovak University of Agriculture in Nitra, Slovak Republic

The objective of this work was to assess the influence of solar radiation on the indoor climatic conditions of the examined hall in the summer and winter season. We focused on the determination of temperature damping of an external wall structure. By comparing the temperature damping of the given wall structure with the recommended value of temperature damping we found that the external wall satisfies the thermal requirements for the summer season. Further increasing of the wall thickness would have no impact on the internal environment quality. The assessment of temperature damping for the winter season does not satisfy this condition. The comparison of both calculation methods did not reveal any significant differences that would influence the overall assessment of the wall structure.

Key words: temperature damping, indoor climatic conditions

The purpose of investigating the thermal stability of rooms is to assess the influence of solar radiation on the increase of internal air temperature of the examined room (Ficker, 2004). The indoor climatic conditions in a building influence the physiological needs of persons and their activity (Priecel, 2007). The determination of temperature damping in structures í expresses the influence of heat absorption capacity in building structures on the fluctuation of internal surface temperature under daily variations in external temperature. It means structure behaviour under a modelled, unstable thermal condition (Vaverka et al., 2006).

The fluctuation of external air temperatures invokes the fluctuation of temperatures in the structure, on the external and internal surface of the building structure (Chmúrny, 2003). The temperature damping of the structure í means the ability of this structure to damp the thermal variations of external surface and specifies how many times the amplitude of internal surface temperature is lower than the amplitude of external air temperature (Vaverka et al., 2006). Temperature damping is determined on the basis of thermal performance of the external cladding structure or its layers (Chmúrny, 2003).

Materials and methods

The temperature damping of the external wall structure was assessed in the mechanised repair workshop Kolíňany. The external masonry of the building is made of light-weight aerated concrete blocks with a thickness of 300 mm; both of its sides are of a lime-cement plaster with a thickness of 15 mm. The composition of the external structure is shown in Figure 1, and the thermal performance of individual layers of the wall is presented in Table 1.

Assessment will be done upon a precise calculation by means of a Fourier equation according to Šklover et al. (1966) and Halahyja et al. (1985), where the outputs are expressed in a complex form. The results of this calculation will be compared with commonly used approximate equations according to

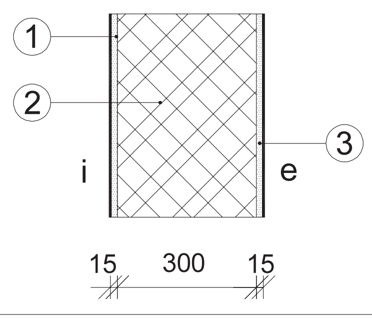

Figure 1 Composition of the external wall structure
1, 3 – lime-cement plaster, 2 – light-weight aerated concrete blocks

Obrázok 1 Skladba obvodovej stenovej konštrukcie
1, 3 – vápenno-cementová omietka, (2) plynosilikátové tvárnice

Table 1 Thermal performance of building materials (STN 73 0540-3)

Layer (1)	Material (2)	Thickness of layer – d in m (3)	Bulk weight – ρ_o in kg/m3 (4)	Coefficient of thermal conductivity – λ in W/(m × K) (5)	Specific heat capacity – c in J/(kg × K) (6)
1.	Lime-cement plaster (7)	0.015	2 000	0.99	790
2.	Light-weight aerated concrete blocks (8)	0.300	550	0.19	840
3.	Lime-cement plaster (9)	0.015	2 000	0.99	790

Tabuľka 1 Teplotechnické vlastnosti stavebných látok (STN 73 0540-3)
(1) vrstva, (2) materiál, (3) hrúbka vrstvy, (4) objemová hmotnosť, (5) súčiniteľ tepelnej vodivosti, (6) tepelná kapacita, (7) vápenno-cementová omietka, (8) plynosilikátové tvárnice, (9) vápenno-cementová omietka

Chmúrny (2003) and Vaverka (2006) with the subsequent assessment.

Specification of temperature damping

A. Fourier equation of temperature damping for a three-layer structure can be expressed in the following form:

$$\theta_e = \frac{s_2}{s_3}\cdot\left[\frac{s_1}{s_2}\cdot N\cdot\cos h\left(\frac{\bar{s}_2}{\lambda_2}\cdot d_2\right) + M\cdot\sin h\left(\frac{\bar{s}_2}{\lambda_2}\cdot d_2\right)\right]\cdot \left[\sin h\left(\frac{\bar{s}_3}{\lambda_3}\cdot d_3\right) + \frac{\bar{s}_3}{h_e}\cdot\cos h\left(\frac{\bar{s}_3}{\lambda_3}\cdot d_3\right)\right] + \left[\frac{s_1}{s_2}\cdot N\cdot\sin h\left(\frac{\bar{s}_2}{\lambda_2}\cdot d_2\right) + M\cdot\cos h\left(\frac{\bar{s}_2}{\lambda_2}\cdot d_2\right)\right]\cdot \left[\cos h\left(\frac{\bar{s}_3}{\lambda_3}\cdot d_3\right) + \frac{\bar{s}_3}{h_e}\cdot\cos h\left(\frac{\bar{s}_3}{\lambda_3}\cdot d_3\right)\right] \quad (1)$$

where:

- λj – oefficient of thermal conductivity for the jth layer, W/(m.K)
- s_j – heat absorption capacity for the jth layer of the structure, W/(m^2.K)
- h^e – coefficient of heat transfer on the external side of the structure, W/(m^2.K), (STN 73 0540-3)
- d_j – thickness of individual layers, m
- M, N – parameter indicating the ratio between the heat flow and thermal amplitude

Taking into account the time period $t = 24$, $h = 86\,400$ s, the following equation shall apply to heat absorption capacity of layers according to Standard STN 73 0540-4:

$$s_j = \sqrt{\frac{2\pi}{t}\cdot\lambda_j\cdot c_j\cdot\rho_j} = 0.00853\cdot\sqrt{\lambda_j\cdot c_j\cdot\rho_j} \quad (2)$$

where:

- c_j – pecific heat capacity, J/(kgxK)
- ρ_j – bulk weight, kg/m^3

Then:

$$\bar{s}_j = s_j\cdot\sqrt{i} \quad (3)$$

The mathematical expression of the parameters specified in Equation (1) is as follows:

$$M = \cos h\left(\frac{\bar{s}_1}{\lambda_1}\cdot d_1\right) + \frac{h_i}{\bar{s}_1}\sin h\left(\frac{\bar{s}_1}{\lambda_1}\cdot d_1\right) \quad (4)$$

$$N = \sin h\left(\frac{\bar{s}_1}{\lambda_1}\cdot d_1\right) + \frac{h_i}{\bar{s}_1}\cos h\left(\frac{\bar{s}_1}{\lambda_1}\cdot d_1\right) \quad (5)$$

The thermal resistance of individual layers will be calculated according to the following equation (Chmúrny, 2003):

$$R = \sum_{j=1}^{n}\frac{d_j}{\lambda_j} = \frac{d_1}{\lambda_1} + \frac{d_2}{\lambda_2} + \frac{d_3}{\lambda_3} \quad (6)$$

In order to determine the structure temperature damping in the summer and winter seasons, the absolute value of temperature damping ν shall be specified in the complex form $\Theta \rightarrow a + bi$, where a is a real part and bi is an imaginary part. The absolute value of temperature damping is determined by means of a complex number modulus:

$$v_L = \mathrm{mod}\Theta = \sqrt{(a^2 + b^2)} \quad (7)$$

Procedure for calculation

1. The thermal resistance of the external wall R will be determined according to Equation (6).
2. The heat absorption capacity of individual layers s_j and $\bar{s}_j$ will be specified according to Equation (2).
3. The values $\cos h(R_j\cdot\bar{s}_j)$ and $\sin h(R_j\cdot\bar{s}_j)$ will be calculated. Here:
   $\cos hR_j\cdot\bar{s}_j = \cos h(y + yi) = \cos hy\cdot\cos y + i\sin hy\cdot\sin y = a + bi$
   $\sin hR_j\cdot\bar{s}_j = \cos h(y + yi) = \sin hy\cdot\cos y + i\cos hy\cdot\sin y = c + di$
   where: $y = \frac{R\cdot s}{\sqrt{2}}$
4. The values M and N will be calculated according to Equations (4) and (5).
5. Temperature damping will be calculated according to Equation (1).
6. The absolute value of temperature damping for the summer season ν_L and for the winter season ν_Z will be calculated according to Equation (7).
7. The minimum values $\nu_{L\,\min}$ or $\nu_{Z\,\min}$ will be determined in accordance with Standard STN 73 0540-4, and assessment will be carried out after that.

B. Temperature damping will be calculated by means of an approximate procedure specified by the standard

Results and discussion

The following results were obtained on the basis of the submitted procedure:

- **Summer season**
  1. Calculation by means of Fourier Equation (1) $\nu_{L1} = 41.76$
  2. Approximate calculation $\nu_{L2} = 37.83$

- **Assessment**
  1. $\frac{\nu_{L1} > \nu_{L\,\min}}{41.76 > 14.89} \rightarrow$ conforms to the condition
  2. $\frac{\nu_{L2} > \nu_{L\,\min}}{37.83 > 14.89} \rightarrow$ conforms to the condition
- **Winter season**
  1. Calculation by means of Fourier Equation (1) $\nu_{Z1} = 39.75$
  2. Approximate calculation $\nu_{Z2} = 35.97$
- **Assessment**
  1. $\frac{\nu_{Z1} > \nu_{Z\,\min}}{39.75 > 44.47} \rightarrow$ fails to conform to the condition
  2. $\frac{\nu_{Z2} > \nu_{Z\,\min}}{35.97 > 44.47} \rightarrow$ fails to conform to the condition

Temperature damping determined in the investigated wall structure in both examined cases satisfies for the summer season the requirements for the minimum value of temperature damping; the recommended values are exceeded more than two times. It means that further increasing of the wall thickness would have no effect as regards the internal environment quality. Because of this reason, it will be necessary to focus on whether the size of transparent surfaces, their qualitative thermal performance, and their orientation towards the compass directions is well-founded in relation to the requirement on the power and placement of a local air-conditioner. The assessment of temperature damping for the winter season is usually not required. In our case, it slightly fails to conform to this requirement.

Conclusions

By comparing the temperature damping of the given wall structure with the recommended value of temperature damping it was discovered that the external wall satisfies the thermal requirements for the summer season. For a comprehensive assessment of the building it is necessary to verify all of the other parts of the building external cladding that are exposed to external environment influence. It was found that the wall is able to contribute significantly to the thermal stability of the assessed internal space. The comparison of both calculation methods did not reveal any significant differences that would influence the overall assessment of the wall structure.

Súhrn

Cieľom práce bolo posúdiť vplyv slnečného žiarenia na vnútornú klímu skúmaného halového objektu v letnom a zimnom období. V práci sme zamerali pozornosť na stanovenie teplotného útlmu obvodovej stenovej konštrukcie. Porovnaním teplotného útlmu danej stenovej konštrukcie s odporúčanou hodnotou teplotného útlmu sme zistili, že obvodová stena vyhovuje teplotechnickým požiadavkám kladeným na letné obdobie. Ďalšie pôsobenie na kvalitu vnútorného prostredia iba zväčšovaním hrúbky steny by už nebolo efektívne. Posúdenie teplotného útlmu pre zimné obdobie podmienke nevyhovuje. Pri porovnaní oboch výpočtových metód neboli zistené významné rozdiely, ktoré by ovplyvnili celkové hodnotenie stenovej konštrukcie.

Kľúčové slová: teplotný útlm, vnútorná klíma

This paper was prepared with the support of research project VEGA 1/0769/10.

References

FICKER, T. 2004. Handbook of building thermal technology, acoustics and daylighting – Příručka stavební tepelné techniky, akustiky a denního osvětlení. 1. vyd. Brno : Akademické nakladatelství CERM, 2004. 266 p. ISBN 80-214-2670-5.

HALAHYJA, M. et al. 1985. Stavebná tepelná technika, akustika a osvetlenie. 1. vyd. Bratislava : ALFA, 1985. 752 s.

CHMÚRNY, I. 2003. Tepelná ochrana budov. 1. vyd. Bratislava : Jaga, 2003. 214 s. ISBN 80-88905-27-3.

PRIECEL, J. – KARANDUŠOVSKÁ, I. – BALKOVÁ, M. 2007. Ploché strechy, ich vady, opravy a rekonštrukcie. In: Construmat 2007: sborník přednášek z XIII. medzinárodní konference. Ostrava : Vysoká škola báňská, Technická univerzita, 2007, s. 238 – 240. ISBN 978-80-248-1536-7.

STN 73 0540-3:2002. Tepelnotechnické vlastnosti stavebných konštrukcií a budov – Tepelná ochrana budov – Vlastnosti prostredia a stavebných výrobkov.

STN 73 0540-4:2002. Tepelnotechnické vlastnosti stavebných konštrukcií a budov – Tepelná ochrana budov – Výpočtové metódy.

ŠKLOVER, A. M. – VASIĽJEV, B. F. – UŠKOV, F. V. 1966. Osnovy strojiteľnoj teplotechniky žilych i obščestvennych zdanij. Moskva: Strojizdat, 1966.

VAVERKA, J. 2006. Stavební tepelná technika a energetika budov. Brno : VUTIUM, 2006. 648 s. ISBN 80-214-2910-0.

Contact address:
doc. Ing. Štefan Pogran, CSc., Department of Structures, Faculty of Engineering, Slovak University of Agriculture in Nitra, Tr. A. Hlinku 2, 949 78 Nitra, e-mail: stefan.pogran@uniag.sk

Acta technologica agriculturae 3
Nitra, Slovaca Universitas Agriculturae Nitriae, 2011, s. 69–73

METHODOLOGY OF PROCESS MODELS CREATION USING THE ENTERPRISE ARCHITECT SOFTWARE TOOL

METODIKA PRO TVORBU PROCESNÍCH MODELŮ POMOCÍ SW NÁSTROJE ENTERPRISE ARCHITECT

Pavel MÁCHAL

Mendel University in Brno, Czech Republic

A continuous improvement of business processes is a must for any company that wants to stay in the market. Customers requiring better and better products and services force all enterprises to think continuously about improving of their business processes. Such an approach is based on a good understanding and measuring of an existing process and, thus, from the resulting stimuli of its improvement. A software (SW) tool called Enterprise Architect enables, among others, to model individual business processes. The main objective of business processes modelling is to create a correct specification of these processes and to analyse their properties. The purpose of business processes modelling is to create such an abstraction of a process which would enable to understand all its activities and all relationships existing between these activities on one hand and roles represented by capabilities of people and facilities involved in a given process. The objective of this paper is to create a uniform methodology of business processes modelling when using the SW tool Enterprise Architect.

Key words: Process model, methodology of modelling, activity, process, modelling area

Process modelling is basically a dynamic image of real business activities displayed via the methods and approaches used for specifying and analysing these processes. Enterprise Architect (hereafter referred to as EA) is a CASE type tool developed by Australian company Sparx Systems. Versions are currently available for MS Windows and Linux platforms. Enterprise Architect is based upon UML version 2.1 support but, along with the ability to define other elements and their features, comes practically unlimited potential for designing the user's own models. It is a tool which can support and greatly facilitate the entire phase of the software development, from defining the system requirements and designing, to preparing test and system documentation. Furthermore, EA supports Business Process Modelling, which is surely an advantage against other CASE tools that support only UML based modelling.

Creating a unified methodology for the process modelling technique designed using EA can subsequently help to provide an efficient business process modelling.

Materials and methods

Business process modelling has experienced a rapid growth over the past few years. It has brought success where previous approaches failed as it provided business strategists and technologists with a unified set of tools and strategies for achieving the common goals. The future promises even more expansive growth and development, mainly due to the global economic crisis and the subsequent need for re-engineering enterprises, businesses and all manner of other institutions.

The EA software itself enables both extensive variety during business process modelling and various interpretations. The author of this contribution created an original methodology and standards for an effective process model using EA. The methodology and standards primarily enable the unified interpretation and comparison of different models designed using the afore-mentioned software tool.

Results and discussion

After the opening of the EA tool a basic screen appears. It is useful to separate the basic screen into three graphic areas. Each of them has a name describing its functions. The areas are as follows: Toolbox, placed on the left side of the screen, Diagram, placed in the middle, and, finally, the third area, Project Browser, on the right side of the screen.

The Toolbox contains tabs with elements that can be dragged into the "Modelling Area" in the middle of the screen. The „Modelling Area", though, serves mainly to display the graphic representation of the constituent processes. A storage site for elements is then automatically created within the "Project Browser". The database content is created in this manner as the elements are filed under the active Package.

These three areas can be switched on, off, widened or narrowed, depending on which area of a model is currently being processed.

When creating a process model, this methodology works with the following practices.

- **Colouring the elements**

This method uses colour distinction of elements. In the final state, the colours improve the legibility and arrangement of diagrams. The colours can be chosen (bottom left corner of the screen) when the cursor is placed on the corresponding element. It is also possible to choose them accumulatively – in the "Modelling Area" by dragging the mouse while holding the left button.

- **Rectangular convention**

To arrange the diagrams neatly it is necessary to use the rectangular convention for the sequence of activities and

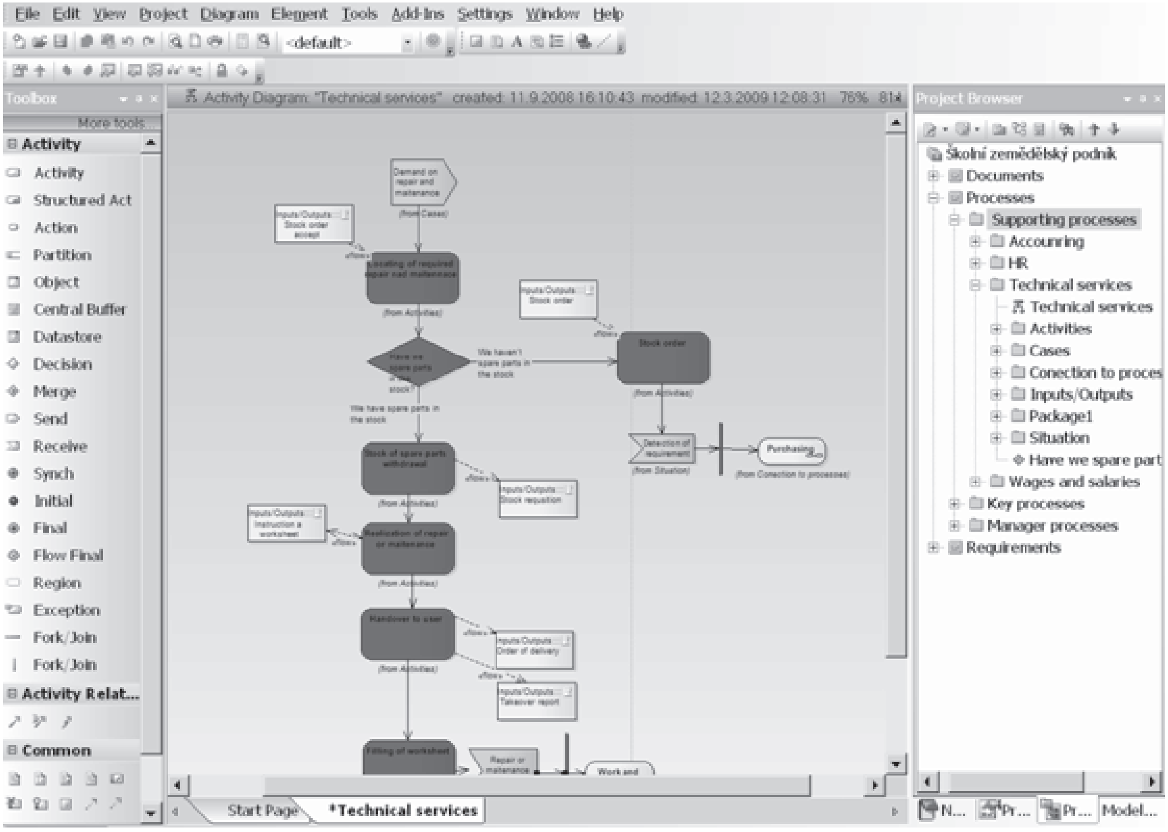

Figure 1 The basic screen of the EA tool
Source: author
Obrázok 1 Vstupní obrazovka EA
Zdroj: Autor

situations. Since the system does not support this convention, it must be done manually. The rectangular convention improves the legibility of diagrams.

- **Element alignment**

After choosing the elements to align (using the right mouse button), the alignment possibilities appear on screen (up, down, right, left). Alternatively, the alignment can be carried out automatically by creating even spaces between the elements – downwards or upwards.

- **One name practice**

In EA a unique identification number is assigned to each established element. This is necessary for the purpose of copying the multiple elements into diagrams. The identification number is assigned to each element automatically, unlike the name that is assigned by the user. When changing the name of an element in the database, all its copies within diagrams are renamed. However, a danger exists in creating (by establishing or copying) an element with the same name but different identification number. In such a case, when used in diagrams, the advantage is lost. Therefore, any element should have only one name and one unique identification number.

- **The principle behind creating packages**

When modelling, it is necessary to create the structure of the packages (in the “Project Browser”) first, so the established elements can be filed within these packages.

Elements filed in such a direct way can be easily and systematically used after the process analysis is completed.

When creating packages and, subsequently, outputs, it is good to know that:

- Elements filed in a package carry their text into the diagrams (“From....”).
- It is possible to import/export whole packages.
- Documentation (HTML, RTF) can be created only from the active package – the package on which the cursor is placed. Only what is saved in the active package will be transferred into the documentation. When creating documentation of the whole model, the highest-level package must be highlighted.

- **Creating Hyperlink**

Graphs can be linked to documents filed in a defined package by dragging the Hyperlink element from the top tool bar and placing it on the relevant element (Output). Double clicking on a file will open it (MS WORD, MS EXCEL…). This is useful for a more detailed description of activities. Furthermore, a relevant document or template can be opened directly when entering/leaving an activity.

- **Creating package**

A new package can be created by clicking the “New package” icon and giving it a name. Deleting is done by the right hand mouse button and choosing Delete. The entire methodology used in the process modelling is based on the package structure.

- **Diagram**

Double clicking on the “New Diagram“ icon will create a diagram. However, a package will be created first and will be assigned the name of the future process. Afterwards, a diagram is established in the empty “Modelling Area”. A diagram established this way would carry the package name.

- **Element**

An element can be created either from the Toolbox, in the case of its being a unique incidence, or from the Project Browser, in the case of its being a repeated incidence. Creating from the Project Browser enables the establishment of a set of diagram elements without their presence in a diagram. These elements can be dragged into the "Modelling Area" using the mouse.

This is how it is established and subsequently placed into the "Modelling Area":
- Actor.
- Artefact.
- Requirement.

The most commonly used elements in process modelling using the EA software

Activity

The element "Activity" is used for an activity description. It is established by dragging the mouse from the Toolbox on the "Activity" tab into the "Modelling Area". The activity is marked green. The heading can contain a short name activity.

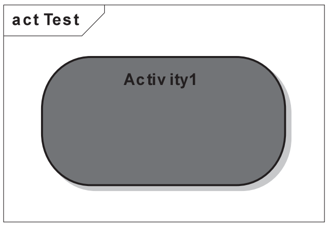

Figure 2 Activity
Source: author
Obrázok 2 Aktivita
Zdroj: autor

Actor

The yellow "Actor" element is used to define a process participant, i.e. the person who carries out the activity. It is placed to the left of the "Activity" and linked with the activity it does through "Relation".

It is necessary to differentiate between a position in an organization chart and a "Role". One position can have many defined roles within one process (e.g. employee, leader). The "Role" is established within the "Project Browser" and can be dragged into the "Modelling Area" by mouse. Individual roles can be dragged by mouse, placed one beneath the other and form a structure of the "roles", which does not appear in the diagram.

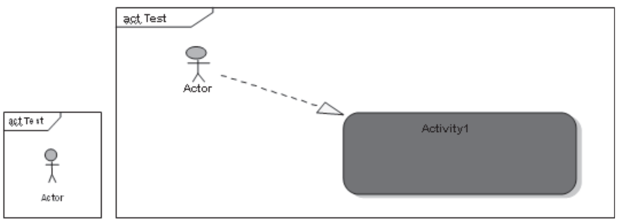

Figure 3 Actor
Source: author
Obrázok 3 Role
Zdroj: autor

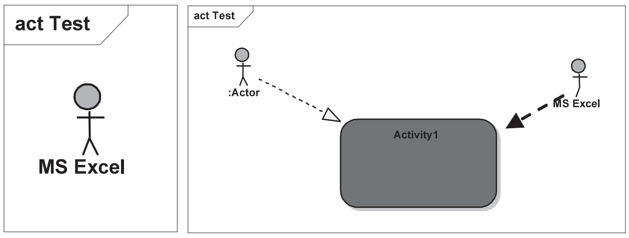

Figure 4 Used application
Source: author
Obrázok 4 Použitá aplikace
Zdroj: autor

Used application

The blue "Actor" element is used to describe the application used for the document related to the activity. It is placed to the right of the "Activity" and is linked via "Relation".

Events

The "Send" element from the "Analysis" tab can be used to express an event (the external activity initiative). Its colour is purple. Such highlighting improves the legibility of the diagram.

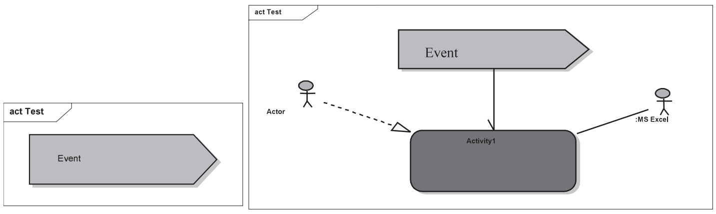

Figure 5 Events
Source: author
Obrázok 5 Události
Zdroj: autor

Status

The "Receive" element from the "Analysis" tab can be used to express status (the internal activity initiative). Its colour is brown. Such highlighting improves the legibility of the diagram.

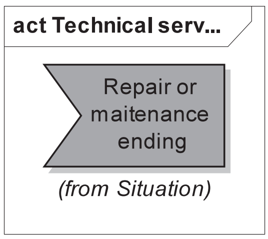

Figure 6 Status
Source: author
Obrázok 6 Stav
Zdroj: autor

Input/Output

The "Artefact" element is used for documents and data objects. It is created by establishing it within the "Project Browser" and can be dragged into the "Modelling Area" by mouse. The colour of this element is blue. The input is to the left and the output to the right. The relation is "Information Flow".

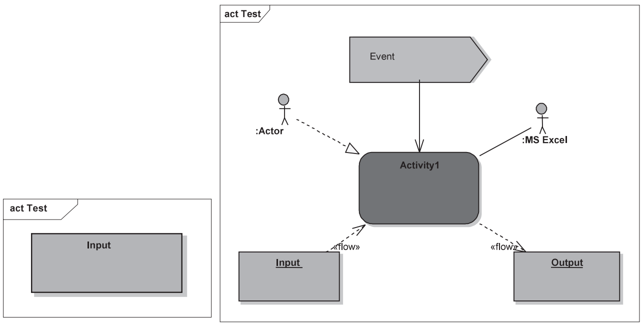

Figure 7 Input/Output
Source: author
Obrázok 7 Vstup/Výstup
Zdroj: autor

Requirement

When the goal of the project is to define, for example, the requirements for IS/IT, the element "Requirement" is established within the "Project Browser". The element can be dragged by mouse onto the desktop and linked with an activity. The requirement is assigned to a specific (concrete) activity in this manner.

The structure of the output document will be formed by moving into other packages and sorting all the requirements prior to creating the documentation.

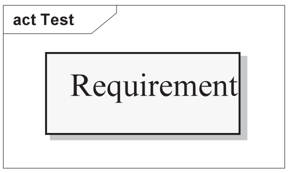

Figure 8 Requirement
Source: author
Obrázok 8 Požadavek
Zdroj: autor

Parallel processes

Parallel processes can be represented by a horizontal or vertical line "Fork/Join" from the "Activity" tab. The "Fork/Join" line represents parallel processes that are independent from each other but must be executed before the process continues. The line can be extended to the necessary length by placing the cursor on the end and pulling with the left mouse button.

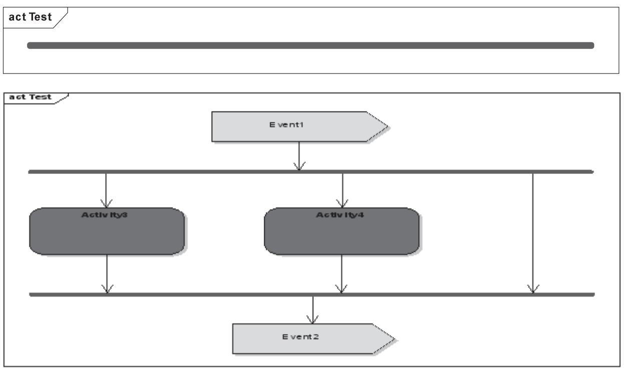

Figure 9 Parallel processes
Source: author
Obrázok 9 Paralelní procesy
Zdroj: autor

Decision-making activities

The "Decision" element from the "Activity" tab is used to bifurcate the process when there is a known condition and the process continues accordingly along one branch or the other. The red colour is used for this condition. The bifurcation condition is placed into the name of the "Control Flow" by double clicking on the line and entering the name. To bend the line it is necessary to click on the line with the right button and choose "Bend Line at Cursor". The black "Merge" element from the "Activity" tab is used to merge processes when the dynamic link returns into the logical flow of the diagram.

Connecting status, activity and other elements in a logical sequence is done by switching on the "Control Flow" on the "Activity" tab followed by dragging the mouse from one element to another (e.g. status – activity). An arrow on the line will respect the direction of drag (logic).

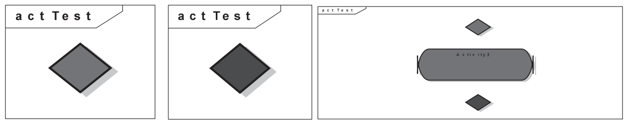

Figure 10 Decision-making activities
Source: author
Obrázok 10 Rozhodovací činnost
Zdroj: autor

Connecting diagrams

After dragging a process symbol (from the "Project Browser") into the "Modelling Area" and choosing Hyperlink, the symbol, representing the process of the given name, will appear. Clicking it enables switching between processes within the diagram and also within the subsequently created HTML documentation.

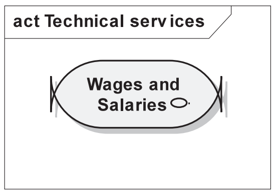

Figure 11 Process
Source: author
Obrázok 11 Proces
Zdroj: autor

General rules for process modelling via the EA software

Deleting unused objects

During modelling, one element can be established both in the "Modelling Area" and in the "Project Browser". When the element is deleted from the "Modelling Area", it remains in the "Project Browser".

The EA software does not have a function for deleting unused elements. It is necessary to use the following procedure:

- open process,
- right click on all the elements, one after the other,
- open the drop down menu and when the text "Locate in Current Diagram" is black, the element also exists in the "Modelling Area". When it is grey, the element does not exist in the "Modelling Area". The "Delete" function deletes the element.

Packages system

During the modelling, all elements are gradually arranged in one file. If the diagram is larger and has a lot of elements, their graphical symbols may be merged.

For that reason, it is necessary to establish the following subsets:

- Events,
- Activities,
- Statuses,
- Linking to processes,
- Inputs/Outputs.

Filing up elements into packages

Elements can be dragged into packages with the mouse. This makes the established elements look neater. The "From..." sign then appears beneath the graphic symbol in the "Modelling Area". This improves the legibility of the diagram.

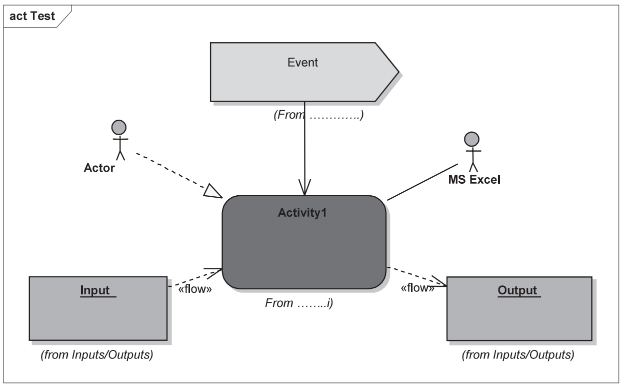

Figure 12 A part of the process after the insertion of elements into packages
Source: author
Obrázok 12 Část procesu po zařazení elementů do složek
Zdroj: autor

Documentation

Icons in the top left corner of the "Project Browser" are used to create the documentation. The documentation can be created in the following formats:

- **HTML**
  Clicking on a package in the "Project Browser" highlights the target package in which the documentation will be created. When the documentation concerns the whole model, the highest-level package should be selected. Thus, the generation begins. The documentation acts in a similar manner to a live system: it is possible to switch between applications and so on.
- **RTF**
  The same rules concerning the work with packages apply to an export into MS WORD – RTF. The difference is that it is necessary to choose a template – the form of the output report. The templates provided can be altered to suit.

Export/Import

When creating a copy of a process or a model, it is recommended to export into "XLM" followed by import from the newly created file. Copies contain all the graphics and are the same as the original.

Export/Import is done by clicking the right mouse button on the relevant package and choosing the Export/Import function.

Conclusions

The purpose of business process modelling is to create a precise specification of the processes and to analyse their features. The intent of business process modelling is to create a process abstraction that enables the understanding of all its activities, the links between these activities and roles represented by the abilities of the people and facilities involved in the process.

There are many approaches and methodologies concerning business process modelling. These are usually created in connection with a software product designated for the process modelling.

The aim of creating this methodology for modelling techniques was to provide the users of Enterprise Architect software with the basic set of terms and rules for their use, so the process model maker could describe all the real behaviour and features in an easy way that does not change.

Souhrn

Zlepšování podnikových procesů je dnes nezbytností pro udržení firmy na trhu. Podniky jsou nuceny svými zákazníky, kteří žádají stále lepší produkty a služby, soustavně uvažovat o zlepšování svých procesů. Tento přístup je založen na porozumění a měření stávajícího procesu a z toho přirozeně vyplynuvších podnětů k jeho zlepšování. SW nástroj Enterprise Architect. Umožňuje mimo jiné modelování obchodních procesů. Hlavním účelem modelování obchodních procesů je vytvoření korektní specifikace procesů a analýzy jejich vlastností. Smyslem modelování obchodních procesů je vytvořit takovou abstrakci procesu, která umožňuje pochopení všech jeho aktivit, souvislostí mezi těmito aktivitami a rolemi reprezentovaných schopnostmi lidí a zařízení zapojených do daného procesu. Cílem příspěvku je vytvořit jednotnou metodiku techniky modelování procesů pomocí nástroje Enterprise Architect.

Klíčová slova: procesní model, metodika modelování, činnost, proces, modelovací plocha

References

ARIS Architecture of Integrated Information System. 2003. Available at: < Methodologies /ARIS/ARIS.HTML>

BPMI Business Process Modeling Notation. Version 1.0 – May 3, 2004. Business Process Management Initiative. Available at: <http://www.bpmi.org>

LINHARTOVÁ, D. 2008. Vysokoškolská psychologie. Brno : MZLU, 2008. 151 s. ISBN 78-80-7375-172-2.

MÁCHAL, P. – LIŠKA, S. 2008. Utilization attribute in procedural simulation at optimum assignation of production process. In: Skoupý, A. – Máchal, P. – Mareček, L. 2008. Proceedings of the 3rd ISC Fortechenvi 2008. Brno : MZLU, 2008. s. 133 – 135. ISBN 978-80-7375-182-1.

ŘEPA, V. 2007. Podnikové procesy – procesní řízení a modelování. Praha : Grada, 2007. 281 s. ISBN 78-80-247-2252-8.

Contact address:
Ing. Pavel Máchal, CSc., Institute of the Lifelong Education, Mendel University of Agriculture and Forestry in Brno, Zemědělská 1, 613 00 Brno, Czech Republic, e-mail: pmachal@mendelu.cz

Acta technologica agriculturae 3
Nitra, Slovaca Universitas Agriculturae Nitriae, 2011, s. 74–78

ASSEMBLY PROCESS CAPABILITY OF AUTOMOTIVE SEATS

SPÔSOBILOSŤ PROCESU MONTÁŽE SEDADIEL AUTOMOBILOV

Zuzana ANDRÁSSYOVÁ, Jozef HRUBEC, Martin KOTUS
Slovak University of Agriculture, Slovakia

The study focuses on the evaluation of assembly process capability of automotive seats according to safety/regulation S/R characteristics defined by organization and ISO 9001: 2008 Quality Management Systems. Requirements. Therefore, there is analysed the statistical process control on the basis of normality and stability of processes and following manufacturing process capability indexes C_p and C_{pk} are calculated. The level of quality is assured with a control system Poka Yoke for each manufacturing process of S/R characteristics, such as screwing of airbag, RSE, safety lock, Isofix, bladder, backrest plus seat. This fact is considered in the results of capability which met the conditions C_p, $C_{pk} \geq 2$ specified by Faurecia.

Key words: automotive seat, control charts, manufacturing process capability C_p and C_{pk}, process stability, Poka Yoke method

The seats of an automobile represent an important part of automotive industry taking into account the quality, safety, comfort, etc. Therefore, it is required to assure the quality of manufacturing process within each production phase. The monitoring and evaluation of manufacturing process capability presents one of the methods for ensuring and improving the processes in manufacturing organization. It includes the monitoring of stability and normality of obtained values from manufacturing processes and the calculation of manufacturing process capability indexes C_p and C_{pk}. The assembling process of first row seats is analysed through the manufacturing processes considering the safety/regulation S/R characteristics in perspective of capability. The manufacturing process of individual S/R characteristics is assured by the Poka Yoke system, i.e. by a 100 % check. “The basic principle of Poka Yoke is to prevent the non-conformities systematically. Using technical tools, modification of a product, fixture, device, etc., the Poka Yoke system enables to register and warn against the non-conformity and, if it is necessary, to stop the manufacturing process immediately” (Andrássyová, 2010).

The objective of this paper is to monitor the manufacturing process capability for every S/R characteristic of seats assembly. Processes will be controlled by the evaluation of control charts for the average $\bar{x}$ and range R (STN ISO 8528: 1995 Shewhart control charts). If the provisions for the evaluation of control charts and for the achievement of manufacturing process capability are not fulfilled, the monitored process shall be subjected to a detailed study immediately and corrective and preventive measures shall be proposed. It is also necessary to follow up the state of the Poka Yoke system which assures the quality of the manufacturing process.

Material and methods

Quality indicators

The S/R characteristics which consider the safety level and legislative requirements of final customer’s country (Figure 1) are defined as the most important indicators taking into account the quality of automotive seats assembly. The screwing process is applied to the components of the first row seats as follows: airbag, back seat equipment – RSE, bladder (USA), safety lock, Isofix, backrest plus seat. The process parameters of screwing the S/R characteristics are introduced in Table 1.

Figure 1 The S/R characteristics of the automotive seat
Obrázok 1 Bezpečnostné charakteristiky automobilového sedadla

Table 1 The process parameters of screwing the S/R characteristics of the automotive seat

	Airbag (1)	RSE (2)	Bladder (3)	Safety lock (4)	Isofix (5)	Backrest plus seat (6)
Screwing torque in Nm (7)	10 ± 1	4.5 ± 0.5	2.5 ± 0.3	34.5 ± 1.5	11 ± 1	34.5 ± 1.5

Tabulka 1 Parametre procesu skrutkovania bezpečnostných charakteristík automobilového sedadla
(1) airbag, (2) sedadlové vybavenie zadnej časti, (3) sedadlový senzorický prvok, (4) bezpečnostný zámok, (5) úchytky – isofix, (6) opierka + sedák, (7) moment skrutkovania

Data collecting

The analysed values of measured parameters are collected from the screwing process of S/R characteristics at approximately hourly intervals (time interval depends on the given S/R characteristic). The values are recorded by the Poka Yoke system directly in the manufacturing process and sampled from the database of measured torque values for analysis. After that, they are separated into subgroups $k = 25$ with the subgroup range $n = 10$. The study below will analyse in details one of the S/R characteristics of the manufacturing process of the automotive seat, namely the safety lock (Table 2). The described procedure is applicable for all remaining S/R characteristics to be monitored during the manufacturing process.

The measured values are used for the calculation of:

- **An average value of a subgroup sample:**

$$\overline{X}_i = \frac{1}{n}\sum_{j=1}^{n} X_{ij} \tag{1}$$

where:

i –1, 2,..., k – sequential number of the subgroup

j –1, 2,..., n – sequential number of the measured value in the subgroup

k – number of subgroups

n – subgroup size

X_{ij} – measured value in the ith subgroup

- **Range in the subgroup:**

$$R_i = \max(X_{ij}) - \min(X_{ij}) \tag{2}$$

where:

$\max(X_{ij})$ and $\min(X_{ij})$ – maximum and minimum value measured in the ith subgroup

The average $\overline{X}_j$ and range R_i are plotted into control charts. The points are linked by lines to visualise the groups and trends.

- **Sample mean of the process:**

$$\overline{\overline{X}}_i = \frac{1}{k}\sum_{i=1}^{k} \overline{X}_i \tag{3}$$

Table 2 Measured values of screwing torque for the safety lock

n	Measured values (1) in Nm												
	1	2	3	4	5	6	7	8	9	10	11	12	13
1	35.07	34.89	34.72	34.75	34.79	34.90	34.76	35.0	34.63	34.76	34.74	34.80	34.80
2	34.69	34.57	34.59	35.09	35.07	34.94	34.68	34.63	34.99	34.63	34.64	34.57	34.85
3	34.66	34.66	34.53	34.75	34.71	34.99	34.79	34.68	34.71	34.75	34.92	34.85	35.0
4	34.69	34.89	34.89	34.68	34.59	34.82	34.72	34.58	34.78	34.96	34.81	34.61	34.85
5	34.62	34.57	34.65	34.52	34.97	34.56	34.64	34.86	34.69	35.08	34.58	34.62	34.61
6	34.98	35.02	34.86	34.57	34.88	34.99	34.56	35.12	34.96	34.61	34.76	34.99	34.70
7	34.85	34.69	34.71	34.88	34.59	34.67	34.61	35.13	34.59	34.84	34.65	34.83	35.01
8	34.73	34.52	34.56	34.88	34.55	34.66	34.76	34.89	34.71	34.87	35.09	34.59	34.75
9	34.59	34.98	34.94	34.78	34.58	35.17	34.56	34.80	34.86	34.78	34.69	34.63	34.97
10	35.04	34.68	34.77	34.80	34.93	34.53	34.54	34.54	34.67	34.58	34.61	34.57	34.58
$\bar{x}_i$	34.79	34.75	34.72	34.77	34.77	34.82	34.66	34.80	34.76	34.79	34.75	34.71	34.79
R_i	0.48	0.50	0.41	0.57	0.52	0.64	0.25	0.59	0.40	0.50	0.51	0.42	0.43

Continuation of Table 2

n	Measured values (1) in Nm											
	14	15	16	17	18	19	20	21	22	23	24	25
1	34.52	34.73	35.10	34.70	34.54	34.59	34.85	34.80	34.89	35.07	34.57	34.69
2	34.64	34.79	34.63	35.09	34.58	34.89	34.87	34.50	34.56	34.64	35.04	34.86
3	34.67	34.89	34.51	35.25	34.70	34.59	35.07	34.94	35.15	34.54	34.81	34.68
4	35.02	34.61	34.61	34.64	34.72	34.89	35.0	34.81	34.63	34.81	35.05	34.76
5	34.52	34.89	34.68	34.59	34.50	34.64	34.52	34.61	34.94	34.89	34.75	34.54
6	34.80	34.52	34.90	34.51	34.71	34.78	34.86	34.81	34.53	34.83	34.84	34.61
7	34.81	34.67	34.95	34.77	34.93	34.71	35.20	34.95	34.85	34.99	34.71	34.78
8	34.67	34.58	34.73	34.61	34.80	34.61	34.54	34.52	34.89	34.57	34.56	34.89
9	34.59	34.60	34.67	34.53	34.70	34.78	34.98	34.83	34.86	34.78	34.61	34.54
10	34.71	34.61	34.53	34.89	34.50	34.95	34.68	34.58	34.60	34.56	34.59	34.50
$\bar{x}_i$	34.69	34.69	34.73	34.76	34.67	34.74	34.84	34.74	34.79	34.77	34.75	34.68
R_i	0.50	0.37	0.59	0.74	0.43	0.36	0.68	0.45	0.62	0.53	0.49	0.39

Tabulka 2 Namerané hodnoty momentov skrutkovania pre bezpečnostný zámok
(1) namerané hodnoty

- **Sample average range:**

$$\overline{R} = \frac{1}{k}\sum_{i=1}^{k} R_i \qquad (4)$$

where:
$\overline{X}_i$, Ri – average and range in the ith subgroup (i = 1, 2,..., k)

- **Upper and lower control limits for the range and average:**
  – for the range:

$$UCL_R = D_4 \cdot R \qquad (5)$$

$$LCL_R = D_3 \cdot R \qquad (6)$$

  – for the average:

$$UCL_{\overline{X}} = \overline{\overline{X}} + A_2 \cdot \overline{R} \qquad (7)$$

$$LCL_{\overline{X}} = \overline{\overline{X}} - A_2 \cdot \overline{R} \qquad (8)$$

where:
A_2, D_3, $D4$ – are the constants of control limits; they are changed depending on the subgroup range from 2 to 25, the values A_2 = 0.308; D_3 = 0.223; D_4 = 1.777 conform to the range n = 10 (STN ISO 8258: 1995; Hrubec, 2009)

Plotting and evaluation of control charts for the average $\overline{X}$ and range R

Calculated values are used for plotting the control charts for the average and range which are analysed and evaluated after that. The manufacturing process is statistically controlled when its variability is caused by random causes only. If the manufacturing process is affected by assignable causes, it is necessary to define the causes of negative effects and also the corrective measures that lead to achievement of the process stability.

Production process capability

We can evaluate manufacturing process capability, if the following conditions are complied:
- process is statistically controlled (stable),
- measured values from the process are featured by the normal distribution,
- technical and other specifications are defined by customer requirements,
- nominal value is located in the centre of the tolerance range.

The capability rates of manufacturing process are presented by the capability indexes C_p and C_{pk}. Before we start to calculate the process capability indexes, the process standard deviation shall be estimated.

- **Estimation of the process standard deviation:**

$$\hat{\sigma} = \frac{\overline{R}}{d_2} \qquad (9)$$

where:
$\overline{R}$ – average range in subgroups
d_2 – constant of a central line; it changes according to the subgroup range (from 2 to 25), the value d_2 = 3.078 corresponds to n = 10; (STN ISO 8258: 1995; Hrubec, 2009)

- **Process capability index C_p:**

$$C_p = \frac{USL - LSL}{6 \cdot \hat{\sigma}} = \frac{T}{6 \cdot \hat{\sigma}} \qquad (10)$$

where:
USL, LSL – upper and lower specification limits
T – tolerance

- **Corrected process capability index C_{pk}:**

$$C_{pk} = \frac{USL - \overline{\overline{X}}}{3 \cdot \hat{\sigma}} \qquad (11)$$

$$C_{pk} = \frac{\overline{\overline{X}} - LSL}{3 \cdot \hat{\sigma}} \qquad (12)$$

Resulting manufacturing process indexes must meet the previously specified condition ($C_p \geq 1.33$ and $C_{pk} \geq 1.33$) which can be corrected by the given organization according to internal requirements (cannot be lower). Faurecia defined this condition of production process capability indexes as follows: $C_p \geq 2$ and $C_{pk} \geq 2$.

Results and discusion

The manufacturing process of screwing the S/R characteristics of the automotive seats was statistically evaluated for the individual parameters of each characteristic. The calculation was carried out by means of Microsoft Excel using the data collected from the manufacturing process by the Poka Yoke system with controls the quality of the seat screwing process. The values from the manufacturing process were featured by the normal distribution according to the criterion of the Pearson´s chi-square test (χ^2). The monitoring and regulation of the manufacturing process were performed along with a nominal value of the characteristic and control limits representing the tolerance for the variability of the characteristic.

The values of the range R_i and primarily their location within the control limits were analysed on the basis of the control chart for the range R. The screwing process of the safety lock (Figure 2) as well as of other evaluated S/R characteristics (airbag, RSE, Isofix, bladder, backrest plus seat) was stable on the basis of analysed variability. Therefore, an evaluation of the control chart for the average $\overline{X}$ for the S/R characteristic of screwing the safety lock as well as other S/R characteristics was approached.

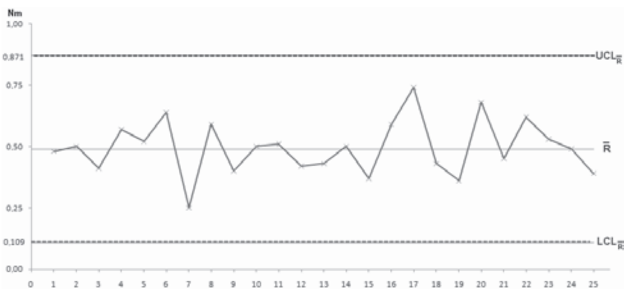

Figure 2 Control chart for the range R, safety lock
Obrázok 2 Regulačný diagram pre rozpätie R, bezpečnostný zámok

Table 3 Calculated values for the defined S/R characteristics in Nm

	Airbag (1)	RSE (2)	Bladder (3)	Safety lock (4)	Isofix (5)	Backrest plus seat (6)
$\overline{\overline{X}}$	10.08	4.53	2.50	34.75	11.03	34.71
$\overline{R}$	0.13	0.07	0.01	0.49	0.07	0.49
UCL_R	0.231	0.124	0.018	0.871	0.124	0.871
LCL_R	0.029	0.016	0.002	0.109	0.016	0.109
$UCL_{\overline{X}}$	10.120	4.552	2.503	34.901	11.052	34.861
$LCL_{\overline{X}}$	10.040	4.508	2.497	34.599	11.008	34.559
C_p	7.892	7.329	30.78	3.141	14.657	3.141
C_{pkh}	7.261	6.889	30.78	2.617	14.217	2.701
C_{pkd}	8.524	7.768	30.78	3.664	15.097	3.581

Tabuľka 3 Vypočítané hodnoty pre definované bezpečnostné charakteristiky v Nm
(1) airbag, (2) sedadlové vybavenie zadnej časti, (3) sedadlový senzorický prvok, (4) bezpečnostný zámok, (5) úchytky – isofix, (6) opierka + sedák

The control chart for the average $\overline{X}$ of the safety lock (Figure 3) shows the position of the manufacturing process taking into account the average value – process mean $\overline{\overline{X}}$. The screwing process of the S/R characteristic was statistically controlled and, therefore, stable. The same result was shown in the control charts for the average $\overline{X}$ and was determined for other S/R characteristics of the seat assembly process.

Resulting from the calculated manufacturing process capability indexes C_p and C_{pk} of screwing the S/R characteristics (Table 3) it is obvious that the manufacturing process capability condition defined by the organization $C_p \geq 2$ and $C_{pk} \geq 2$ is met.

The lowest capability indexes were reached in case of the screwing process of safety lock $C_p = 3.14$, $C_{pk} = 2.62$ (As the lower value of index C_{pk} is always considered for the evaluation, we did not respect the value $C_{pkd} = 3.66$.) and backrest plus seat $C_p = 3.14$, $C_{pk} = 2.7$. The highest capability indexes were reached in case of the screwing process of bladder $C_p = 30.78$, $C_{pk} = 30.78$. These results were achieved with support of applied Poka Yoke method for the quality control that ensured the 100 % check of the manufacturing process. All S/R characteristics of the assembly process for automotive seats in Faurecia are ensured by the Poka Yoke system (Andrássyová, 2010).

Shigeo Shingo (1988) considers the statistical process control (SPC) of taken samples a kind of estimation because of discrepancy of real process behaviour and tolerance of the certain level of non-conformities. The Poka Yoke method discovers the non-conformity in a sub-process and thus prevents the production of non-conforming products. Kaplík (2010) formulates that Visteon Interiors Slovakia, s.r.o. uses the Poka Yoke method to induce the non-conformity intentionally (an insertion of non-conformed part of door panels). A machine must show the failure; otherwise, the

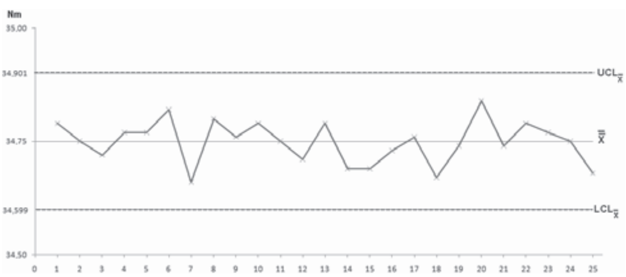

Figure 3 Control chart for the average $\overline{X}$, safety lock
Obrázok 3 Regulačný diagram pre priemer $\overline{X}$, bezpečnostný zámok

sensor is failed and a repair shall be performed. The stability and capability of the manufacturing process is a supportive control tool along with the Poka Yoke system (especially in case of Poka Yoke failure or its ineffective design).

According to Šesták (2006), a qualified evaluation of control charts is more difficult than their structure itself. The analysis of causes (random, assignable) and their effects on the manufacturing process is an important part of the process monitoring. It is necessary to seek interactions of individual elements and move beyond the present knowledge of manufacturing processes behaviour.

Conclusions

The methods of statistical process control and the evaluation of manufacturing process capability verify an ability of the process (together with related circumstances) to meet the defined requirements of product quality (PPM, % non-conformities, reliability, etc.) stably. The Poka Yoke method prevents the non-conformities exactly in the process, so it eliminates the production of non-conformed final outputs. The interaction of these approaches in quality control allows achieving the 100 % quality control and monitoring of process behaviour in a period of time. The production quality is ensured also by other tools and methods of quality control implemented in the organization (Quick Response Quality Control QRQC, Eight Disciplines 8D, 1. OK produced part, etc.); therefore, it is necessary to assess their efficiency, or suggest another approach in the usage of tools and methods in quality control.

Súhrn

Štúdia sa zaoberá vyhodnotením spôsobilosti výrobného procesu sedadiel automobilov na základe bezpečnostných charakteristík definovaných organizáciou a ISO 9001: 2008 Systémy manažérstva kvality. Požiadavky. Štatistická regulácia procesu zahŕňa sledovanie normality, stability výrobného procesu a výsledný výpočet indexov spôsobilosti procesu C_p a C_{pk} montáže automobilového sedadla. Vo výrobnom procese skrutkovania – airbag, RSE, Isofix, bladder, opierka+sedák je kvalita zabezpečená kontrolným systémom Poka Yoke pre jednotlivé bezpečnostné charakteristiky. Táto skutočnosť je zohľadnená aj vo výsledkoch spôsobilosti výrobného procesu, ktoré splnili podmienku C_p, $C_{pk} \geq 2$ stanovenú organizáciou Faurecia, s.r.o.

Kľúčové slová: automobilové sedadlo, regulačné diagramy, spôsobilosť výrobného procesu C_p a C_{pk}, stabilita procesu, metóda Poka Yoke

The results obtained within research project VEGA 1/0576/09 (2009 – 2011) – "The quality improvement of agricultural machines and production systems" were used in this paper.

References

ANDRÁSSYOVÁ, Z. – HRUBEC, J. 2010. Dosahovanie nulovej kontroly kvality zavedením metódy Poka Yoke. In: Kvalita a spoľahlivosť technických systémov. Medzinárodná vedecká konferencia. 25. – 26. 5. 2010, Nitra : SPU, 2010. s. 27 – 31. ISBN 978-80-552-0390-4.

HRUBEC, J. – VIRČÍKOVÁ, E. et al. 2009. Integrovaný manažérsky systém. Nitra : SPU, 2009. 543 s. ISBN 978-80-552-0231-0.

KAPLÍK, P. – BURDA, M. – KORENKO, M. 2010. Zlepšovanie kvality vo výrobnej organizácii prostredníctvom metódy Poka Yoke. In: Medzinárodná vedecká konferencia mladých. 22. – 23. 9. 2010, Nitra : SPU, 2010. ISBN 978-80-552-0441-3.

ŠESTÁK, M. 2008. Riešenie chybovosti a jej príčin na pracovisku. In: Kvalita, roč. 16, 2008, č. 1, s. 11 – 14. ISSN 1335-9231.

SHINGO, S. 1988. Poka Yoke. Improving product quality by preventing defects. [online]. USA : Productivity Press, 1988. p. 282. ISBN 0-915299-31-3. Available at: <http://books.google.sk/books?id=hR_8Ulz6d_oC&printsec=frontcover&dq=poka+yoke&source=bl&ots=kXVhWHmKdD&sig=ynHdsTPwqFAU82kK39Z2qqUYpnI&hl=sk&ei=nhJxS8LPFZjKmgOVoYyRCw&sa=X&oi=book_result&ct=result&resnum=13&ved=0CDUQ6AEwDA#v=onepage&q&f=false>.

STN EN ISO 9001: 2009. Quality management systems. Requirements. SR: Slovak Standards Institute (SUTN).

STN ISO 8258: 1995 (010271). Shewhart control charts. SR: Slovak Standards Institute (SUTN).

Tools of quality assurance. 2010. Internal documentation. FAURECIA Slovakia, s. r. o., JIT Plant Lozorno.

Contact address:
Ing. Zuzana Andrássyová, Slovak University of Agriculture, Faculty of Engineering, Department of Quality and Engineering Technologies, Tr. A. Hlinku 2, 949 76 Nitra, Slovakia

Acta technologica agriculturae 3
Nitra, Slovaca Universitas Agriculturae Nitriae, 2011, s. 78–81

STRESSES IN THE THREE-LAYER SANDWICH BOARDS

NAPÄTOSŤ V SENDVIČOVÝCH TROJVRSTVOVÝCH PANELOCH

Jozef PRIECEL, Milada BALKOVÁ, Dušan PÁLEŠ
Slovak University of Agriculture in Nitra, Slovakia

Three-layer sandwich boards compose boundary layers from fibrocement plates and middle layer from foamy polystyrene. The boundary layers carry bending and normal stresses and the middle layer carries shear stresses. Except shear transfer the polystyrene satisfies the function of thermal isolation too. Two functions of the material may result to economy savings. Simple supported beam was assumed, resisted to continuous load and pressure axial force, with section as the three-layer sandwich board. The relations for calculation of the bending, normal and shear stresses were acquired in the paper. Specificity of computation consists in change of stresses in contact of different materials. The derived formulas were employed for numerical example with assignment of particular values of quantities. Multi-layer boards are essentially more difficult for calculation of stresses.

Key words: sandwich board, bending stress, normal stress, shear stress

In the paper we deal with theoretical principles of the solution of three-layer boards, which boundary layers form fibrocement plates of type Minerit or Cemvin. Basic properties of these plates are sufficient strength, incombustibility, long period of service and non-corrosion. The deficiency is higher absorbability, which assumes safety against direct moisture, mainly using for roof structures. As protection asphalt paperboard or foils may be used. The plates are produced to 18 mm of thickness.

Middle layer of the boards can be foamy polystyrene, which have sufficient strength to transfer of shear stresses. In the case of the insufficient strength is needed his bracing with wood diaphragms. The contact area between the middle layer and the boundary layers is created by glued joint from bitumen glues. The strength of the glue has to satisfy shear strength of the glued materials.

Material and methods

Theoretical principles and analysis

We assume three-layer board, which forms section of simple supported beam with theoretical width 1 m, as it is drawn on the Figure 1. The thicknesses of boundary fibrocement plates are on the figure denoted d and middle layer is described with letter h.

On the beam works general load q and pressure axial force *N*. In arbitrary section *x* arise bending moment *M*(*x*), normal force $N(x)$ and shear force $T(x)$. Step by step we express stresses in section x from these internal forces.

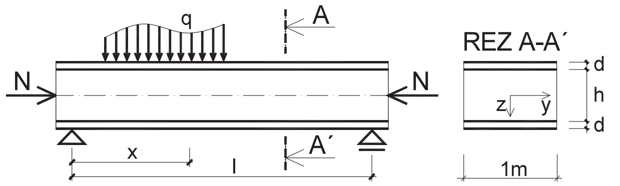

Figure 1 Simple supported beam with the section of the three-layer sandwich board
Obrázok 1 Prostý nosník s prierezom trojvrstvového sendvičového panelu

Results and discussion

Bending moment in the section x – $M(x)$

We exploit the known formula from the elasticity theory for bending stress σ:

$$\sigma = M(x) / J_y \cdot z, \quad \text{Pa} \tag{1}$$

where:
$M(x)$ – bending moment in the section x of beam, N.m
J_y – moment of inertia of the section to axis y, m^4
z – distance of fibre of the section from neutral axis, m

Moment of inertia of compound section J_y we determine as sum of moments of inertia of parts that form a cross – section:

$$J_y = J_{y1} + J_{y2}, \ m^4 \tag{2}$$

where:
J_{y1} – moment of inertia of the boundary plates, m^4
J_{y2} – moment of inertia of the middle layer, m^4

According to Figure 1 partial moments of inertia J_{y1} and J_{y2} can be expressed:

$$J_{y1} = 2 \cdot (1 / 12 \cdot 1 \cdot d^3 + \mathrm{d} \cdot 1 \cdot (h / 2 + d / 2)^2) \tag{3}$$

$$J_{y2} = 1 / n \cdot 1 / 12 \cdot 1 \cdot h^3 \tag{4}$$

In formula (4) is entered factor n reflecting by ratio of modules of elasticity the different materials creating compound section:

$$n = \mathrm{E}_1 / E_2 \tag{5}$$

where:
E_1 – modulus of elasticity of the boundary plates, Pa
E_2 – modulus of elasticity of the middle layer, Pa

From the form (1) we can calculate normal stresses in bending for individual fibres of section, while on joint of boundary layer and middle layer have to hold:

$$\sigma_{z2'} = \sigma_{z2} / n, \ \text{Pa} \tag{6}$$

In neutral axis, in middle of the middle layer, is the stress from bending zero. Development of the stresses σ shows Figure 2.

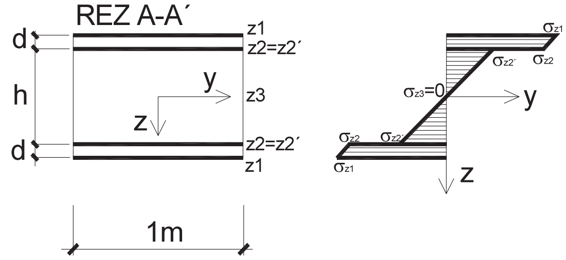

Figure 2 Development of normal stresses from bending moment in the three-layer sandwich board
Obrázok 2 Priebeh normálových napätí od ohybového momentu v trojvrstvovom sendvičovom paneli

Normal force in the section x – $N(x)$

We go out from condition of identity of relative deformation on joint of boundary plates and middle layer:

$$N_1(x) / (A_1 \cdot E_1) = N_2(x) / (A_2 \cdot E_2) \tag{7}$$

Second equation for calculation $N_1(x)$ and $N_2(x)$ is summary condition of equivalence:

$$N(x) = N_1(x) + N_2(x) \tag{8}$$

where:
$N(x)$ – total normal force in the section x, N
$N_1(x)$ – part of the normal force functioning on the boundary plates, N
$N_2(x)$ – part of the normal force functioning on the middle layer, N
A_1, A_2 – areas of the boundary plates and the middle layer, m^2
E_1, E_2 – corresponding modules of elasticity, Pa

We solve then two equations about two unknown quantities and final stresses we calculate by equations:

$$\sigma_1(x) = N_1(x) / A_1; \qquad \sigma_2(x) = N_2(x) / A_2 \tag{9}$$

Development of stresses from the normal force shows Figure 3.

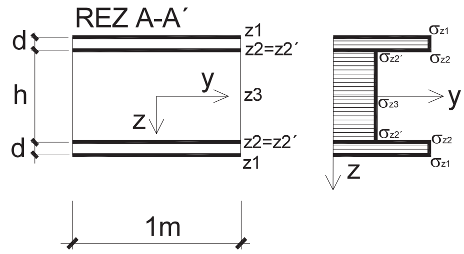

Figure 3 Development of normal stresses from normal force in the three-layer sandwich board
Obrázok 3 Priebeh normálových napätí od normálovej sily v trojvrstvovom sendvičovom paneli

Shear force in the section x – $T(x)$

For shear stress τ the elasticity theory applies:

$$\tau = (T(x) \cdot S_y) / (b \cdot J_y), \ \text{Pa} \tag{10}$$

where:

$T(x)$ – shear force in the section x, N
S_y – static moment of area above fibre of section to gravity centre axis, m^3
b – section width – in our expression unit, m
J_y – moment of inertia of the compound section, m^4

Shear stress according to height of section is represented on the next Figure 4. Its values are:

$$\tau_{z1} = 0;\ \tau_{z2} = (T(x) \cdot S_{yz2}) / (b \cdot Jy) \quad (11)$$

where:

$$S_{yz2} = d \cdot 1 \cdot (h / 2 + d / 2) \quad (12)$$

Between points $z1$ and $z2$ as well as between points $z2'$ and $z3$ will have stress according to section development of quadratic parabola. For determination of shear stress in point $z2'$ we use condition of equality of angular slews in points $z2$ and $z2'$. By help of coefficient m, which gives in relation (13) to ratio the modules of shear of boundary plates and middle layer.

$$m = G_1 / G_2 \quad (13)$$

the shear stress in point $z2'$ is expressed:

$$\tau_{z2'} = \tau_{z2} / m \quad (14)$$

In point $z3$ of section is the shear stress:

$$\tau_{z3} = (T(x) \cdot S_{yz3}) / (b \cdot J_y) \quad (15)$$

where:

$$S_{yz3} = d \cdot 1 \cdot (h / 2 + d / 2) + 1 \cdot h\ /2 \cdot h\ /4 \cdot 1 / m \quad (16)$$

is static moment above neutral axis in the middle of section.

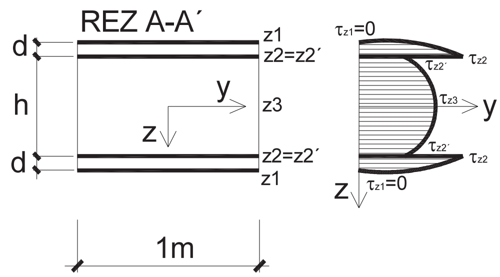

Figure 4 Development of shear stresses from shear force in the three-layer sandwich board
Obrázok 4 Priebeh šmykových napätí od priečnej sily v sendvičovom trojvrstvovom paneli

Numerical example

We employ formulas introduced above for substitution of specific numerical values and we calculate corresponding stresses from each of the three internal forces.

As material for the boundary plates we chose fibrocement plates Minerit and middle layer we designed from foamy polystyrene.
Input values into numerical example then are:

$$E_1 = 8\,000 \text{ MPa};\ \mu_1 = 0.6;\ d = 18 \text{ mm} \quad (17)$$

$$E_2 = 2 \text{ MPa};\ \mu_2 = 0.62;\ h = 120 \text{ mm} \quad (18)$$

where:
E_1, E_2 – modulus of elasticity of Minerit and foamy polystyrene, MPa
μ_1, μ_2 – Poisson´s numbers of materials
d, h – thicknesses of layers according to figures, mm

The applied internal forces are:

$$M(x) = 10 \text{ N} \cdot \text{m};\ N(x) = 500 \text{ N};\ T(x) = 500 \text{ N} \quad (19)$$

For the ratio of modulus of elasticity the relation (5):

$$n = E_1 / E_2 = 8\,000 / 2 = 4\,000 \quad (20)$$

Moments of inertia according to formulas (3), (4), (2):

$$J_{y1} = 2 \cdot (1/12 \cdot 1 \cdot d^3 + \text{d} \cdot 1 \cdot (h / 2 + d / 2)^2) = \quad (21)$$
$$= 2 \cdot (1/12 \cdot 1 \cdot 183 + 18 \cdot 1.\ (60 + 9)2) = 172\,368 \text{ mm}^4$$

$$J_{y2} = 1 / \text{n} \cdot 1 / 12 \cdot 1 \cdot h^3 = \quad (22)$$
$$= 1 / 4\,000 \cdot 1 / 12 \cdot 1 \cdot 120^3 = 36 \text{ mm}^4$$

$$J_y = J_{y1} + J_{y2} = 172\,368 + 36 = 172\,404 \text{ mm}^4 \quad (23)$$

And at last the stresses from the bending moment in the individual points of section from relations (1) and (6):

$$\sigma_{z1} = M(x) / J_y \cdot z_1 = 10\,000 / 172\,404 \cdot (60 + 18) = \quad (24)$$
$$= 4.524257 \text{ MPa}$$

$$\sigma_{z2} = M(x) / J_y \cdot z_2 = 10\,000 / 172\,404 \cdot 60 = \quad (25)$$
$$= 3.480\,198 \text{ MPa}$$

$$\sigma_{z2'} = \sigma_{z2} / n = 3.480\,198 / 4\,000 = 0.00087 \text{ MPa} \quad (26)$$

$$\sigma_{z3} = 0 \text{ MPa} \quad (27)$$

Area of the Minerit A_1 and the foamy polystyrene A_2 in the section:

$$A_1 = d \cdot 1\,000 \cdot 2 = 36\,000 \text{ mm}^2 \quad (28)$$

$$A_2 = h \cdot 1\,000 = 120\,000 \text{ mm}^2 \quad (29)$$

Two equations of two unknown quantities for the normal forces (7), (8):

$$N_1(x) / (A_1 \cdot E_1) = N_2(x) / (A_2 \cdot E_2);\ N_1(x) / \quad (30)$$
$$/ (36\,000 \cdot 8\,000) = N_2(x) / (120\,000 \cdot 2)$$

$$N(x) = N_1(x) + N_2(x);\ 500 = N_1(x) + N_2(x) \quad (31)$$

And of these is $N_1(x) = 499.583680$ N and $N_2(x) = 0.41632$ N. Resulting stresses from the normal force are (9):

$$\sigma_{z1} = \sigma_{z2} = N_1(x) / A_1 = 499.583680 / 36\,000 = \quad (32)$$
$$= 0.013877 \text{ MPa}$$

$$\sigma_{z2'} = \sigma_{z3} = N_2(x) / A_2 = 0.41632 / 120\,000 = \quad (33)$$
$$= 3.469333 \cdot 10^{-6} \text{ MPa}$$

For stresses from the shear force we calculate at first shear modulus G_1 and G_2:

$$G_1 = E_1 / (2 \cdot (1 + \mu_1)) = 8\,000 / (2 \cdot (1 + 0{,}6)) = \quad (34)$$
$$= 2\,500 \text{ MPa}$$

$$G_2 = E_2 / (2 \cdot (1 + \mu_2)) = 2 / (2 \cdot (1 + 0.62)) = \quad (35)$$
$$= 0.617284 \text{ MPa}$$

Shear modulus ratio from the expression (13):

$$m = G_1 / G_2 = 2\,500 / 0.617284 = 4\,049.999676 \quad (36)$$

Resulting shear stresses in the individual points of section by formulas (11), (12), (14), (15), (16):

$$\tau_{z1} = 0 \text{ MPa} \quad (37)$$

$$\tau_{z2} = (T(x) \cdot S_{yz2}) / (b \cdot J_y) = (500 \cdot 1\,242) / / (1 \cdot 172\,404) = 3.602005 \text{ MPa} \quad (38)$$

$$S_{yz2} = d \cdot 1 \cdot (h / 2 + d / 2) = 18 \cdot 1 \cdot (60 + 9) = 1\,242 \text{ mm}^3 \quad (39)$$

$$\tau_{z2'} = \tau_{z2} / m = 3.602005 / 4\,049.999676 = 0.000889 \text{ MPa} \quad (40)$$

$$\tau_{z3} = (T(x) \cdot S_{yz3}) / (b \cdot J_y) = (500 \cdot 1\,242.444444) / / (1 \cdot 172\,404) = 3.603294 \text{ MPa} \quad (41)$$

$$S_{yz3} = d \cdot 1 \cdot (h / 2 + d / 2) + 1 \cdot h / 2 \cdot h / 4 \cdot 1 / m = = 18 \cdot 1 \cdot (60 + 9) + 1 \cdot 60 \cdot 1 / 4\,049.999676 \cdot 30 = = 1\,242.444444 \text{ mm}^3 \quad (42)$$

Conclusion

The presented theoretical results may be used for solution of stresses in critical sections of sandwich boards. Some authors show cases of soft middle layers, in which with bending and pressure or tension are stressed only the boundary layers. Shear stresses transfers then only middle layer. Thereby the calculation simplifies. In supports of the simply supported beam are the maximal shear forces and so the biggest shear stresses too. On the contrary in the middle of span is the maximal bending moment and so the biggest bending stresses too. In the total analysis of stresses is recommended intermediate section, where are manifested the bending, pressure or tension stresses and shear stresses too.

Súhrn

Trojvrstvový sendvičový panel sa skladá z okrajových vrstiev z vlákno-cementových dosiek a zo strednej vrstvy z penového polystyrénu. Okrajové vrstvy prenášajú ohybové a normálové napätia a stredná vrstva prenáša šmykové napätia. Okrem prenosu šmykových napätí môže polystyrén slúžiť tiež ako tepelná izolácia. Dvojitá funkcia strednej vrstvy poskytuje ekonomické výhody. Uvažujeme jednoducho uložený nosník zaťažený spojitým zaťažením a tlakovou normálovou silou, ktorého priečny rez tvorí trojvrstvový sendvičový panel. V článku sme odvodili vzťahy pre výpočet ohybových, normálových a šmykových napätí. Zvláštnosť výpočtu spočíva v zmene napätí na styku okrajovej a strednej vrstvy z rôznych materiálov. Získané vzťahy sme použili na vyčíslenie numerického príkladu s dosadením konkrétnych hodnôt. Viacvrstvové panely sú podstatne zložitejšie pre výpočet napätí.

Kľúčové slová: sendvičový panel, ohybové napätie, normálové napätie, šmykové napätie

Acknowledgement

This research performed at the Department of Buildings of the Faculty of Engineering of the Slovak University of Agriculture in Nitra was supported by the Slovak Grant Agency for Science under grant VEGA no. 1/0013/09.

References

DUNDROVÁ, V. – KOVAŘÍK, V. – ŠLAPÁK, P. 1965. Teória ohybu sendvičových dosiek, Praha.

HOŘEJŠÍ, J. – ŠAFKA, J. 1987. Statické tabulky, Praha : SNTL.

KAISER, J. – SLOŽKA, V. – DICKÝ, J. – JURASOV, V. 1990. Pružnosť a plasticita I. Bratislava : Alfa. ISBN 80-05-00579-2.

KOVAŘÍK, V. 1957. Přibližné metody v rovinné pružnosti. Praha : SNTL.

PÁLEŠ, D. – PRIECEL, J. – VERNAREC, J. – ŠVEC, O. 2008. Optimalizácia geometrického tvaru lomeného oblúka zaťaženého vlastnou tiažou. In: International Science Conference: Rural buildings 2008, Nitra, 18. 9. 2008, s. 76 – 79. ISBN 978-80-227-2941-3.

PÁLEŠ, D. – PRIECEL, J. – VERNAREC, J. – ŠVEC, O. 2008. Optimalizácia geometrického tvaru lomeného oblúka zaťaženého snehom. In: International Science Conference : Rural buildings 2008, Nitra, 18. 9. 2008, s. 80 – 82. ISBN 978-80-227-2941-3.

PRIECEL, J. 1982. Použitie plastov na obalové a strešné konštrukcie poľnohospodárskych stavieb, Thesis, Nitra : SPU.

PRIECEL, J. – PÁLEŠ, D. – BALKOVÁ, M. – ŠVEC, O. 2009. Výpočet sendvičovej dosky s ľahkým jadrom teóriou druhého rádu, International Conference : Construmat 2009, 8. – 10. 6. 2009, Kruh u Jilemnice, Praha, s. 299 – 305. ISBN 978-80-01-04355-4.

RABINOVIČ, A. L. 1946. Ustojčivosť obšivky s zapolnitem pri sžatii. Moskva : Oborongiz.

Contact address:

doc. Ing. Jozef Priecel, CSc., Ing. Milada Balková, PhD., Ing. Dušan Páleš, CSc., Department of Buildings, Faculty of Engineering, Slovak Agricultural University, Tr. A. Hlinku 2, 949 76 Nitra, Slovakia

Acta technologica agriculturae 3
Nitra, Slovaca Universitas Agriculturae Nitriae, 2011, s. 82–84

WELD STRENGTH OF A PACKAGING MATERIAL IN PACKAGING MEDICAL PRODUCTS

PEVNOSŤ ZVARU OBALOVÉHO MATERIÁLU PRI BALENÍ ZDRAVOTNÍCKYCH VÝROBKOV

Stanislav ZEMAN, Martin PRŠAN, Magdaléna VALŠÍKOVÁ
Slovak University of Agriculture in Nitra, Slovakia

The objective of this work was to determine the weld strength of the investigated packaging materials used in packaging medical products. The lap joints of the packaging materials were welded using a discontinuous, indirect welding machine at the pressure of 0.5 MPa. The weld strength is influenced by the temperature of the welded material, the welding time, and the pressure of weld jaws. Based on the evaluated measurements the best weld strength was found in welding the packaging material ED – FLEX NO 058 – 100 – FM with a sterile paper STERIKRAFT D.

Key words: weld strength, welding temperature, tensile machine

Packaging as a means of transport and storage neutralises by its properties temporal, spatial and content-based frictions and fills the space between the production and consumption of goods.

In the packaging of products, it is advisable to consider a more comprehensive optimisation model that would reflect an optimum solution concerning the packaging method for a wide scope of products or for certain groups of products with similar requirements on packaging, having regard to all important functional requirements. Methodically, it is attributing instructions for packaged products to the corresponding properties of a certain packaging and packaging practices. The mathematical solution of such optimisation problems is usually based on linear programming. A prerequisite for a wider application of optimisation methods in packaging is particularly a quantitative statement of considered evaluation criteria which is still quite difficult in most products.

There are specific requirements imposed on packaging; packaging must also meet the conflicting requirements, such as resistance to heat in sterilisation, cooking and freezing, good barrier properties, as well as a minimum impact on the environment (Čurda, 2001).

Such requirements are considered justified as regards the importance for mechanical stresses in transport and consumer packaging and transport packaging units. Unless transport packaging units are sufficiently strong, they will be unable to provide an adequate protection for the packaged product, and it is impossible to expect a trouble-free transport (Lukáš, 1990; Zeman, 2008; Růžička, 1988).

Weldability or the quality of welded joints is significantly influenced by the degradation of plastics by ultraviolet radiation or thermal oxidation. Stabilisers in plastics protect plastics from their effects, however, the ageing process supported by such influences continues. This is the reason for protecting plastic products in order to preserve their bonding ability by welding (Martinec, 1989, 1991; Nemcová, 1996; Štaudner, 1984).

Materials and methods

Welding values must be reviewed periodically in order to ensure the optimum weld quality. When welding is performed by overlapping, it is necessary to observe the relationship between the seam width and material thickness specified in Standard STN 77 0140. The weld jaws with a permanently heated heater were used for welding. The weld pressure was constant, at 0.5 MPa. Experimental measurements were performed using the UltraTest Mecmesin tensile machine (Figure 1), and the sliding speed of gripping jaws was 250 mm.min^{-1}. The measured values were statistically evaluated, and the optimum welding conditions were subsequently determined.

Figure 1 Tensile machine
Obrázok 1 Trhací stroj

In measurements, we used the following packaging materials that are used for packaging medical products:

- Foil EK – FLEX NO 050 – 100 – FM – a packaging material consisting of polyamide with a thickness of 50 μm and polyethylene 100 μm thick, weight per unit area of 149 g.m^{-2}, and water vapour permeability of 18 cm^{3}.m^{-2}.d^{-1}.0.1 MPa^{-1}. The foil is not harmful to health.
- Foil ED – FLEX NO 030 – 070 – FM – a packaging material composed of polyamide with a thickness of 30 μm and polyethylene 70 μm thick, weight per unit area of 98 g.m^{-2}, and water vapour permeability of 30 cm^{3}.m^{-2}.d^{-1}.0.1 MPa^{-1}. The foil is not harmful to health.

- Sterile paper STERIKRAFT D – a packaging material with a thickness of 90 μm, weight per unit area of 69.6 g.m^{-2}, pressure strength of 350 kPa, and air permeability of 465 cm^{3}.m^{-2}.d^{-1}.0.1 MPa^{-1}.

Results and discussion

The objective of experimental measurements was to assess the effect of temperature on the weld strength in packaging medical products. The temperature of welding packaging materials, that usually affects the weld strength, was determined in all experimental measurements. The results of experimental measurements obtained from welding the packaging material EK – FLEX NO 050 – 100 – FM with the sterile paper STERIKRAFT D were evaluated using the analysis of variance. The results of the one-way analysis of variance are shown in Table 1, at significance level $\alpha = 0.05$. We reject the hypothesis of equal means of force under different temperatures. The result of the analysis will determine the effect of each factor separately, or the magnitude of impact the interactions of these factors have on the weld strength. The statistical evaluation of the weld strength for the packaging foil EK – FLEX NO 050 – 100 – FM welded with the sterile paper STERIKRAFT D shows that the weld strength increases with increasing temperature from 1.78 N.15 mm^{-1} to 4.36 N.15 mm^{-1} (Table 2). The Tukey's HSD test of contrasts was used to determine differences in force, and individual homogeneous groups were created. The process of welding is evaluated in Figure 2.

The results obtained during welding the packaging material ED – FLEX NO 030 – 070 – FM with the sterile paper STERIKRAFT D were evaluated using the analysis of variance. These results were tested by the one-way analysis of variance under different temperatures at significance level $\alpha = 0.05$ (Table 3, 4). The Tukey's HSD test of contrasts was used to determine differences in force, and individual homogeneous groups were created. Based on the obtained results it is possible to state that the weld strength achieved at 125 °C was 1.86 N.15 mm^{-1}. It was revealed by comparing the measured values (Table 2) that the difference in weld strength is almost equal. The gradual increasing of temperature from 125 °C to 131 °C caused that the weld strength increased from 1.86 N.15

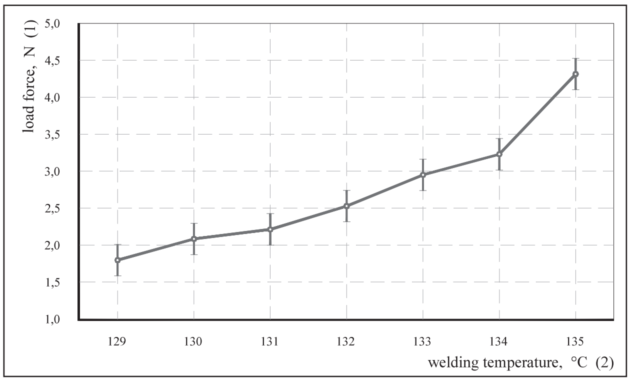

Figure 2 Graph of load force versus welding temperature. Decomposition of effective hypothesis

Obrázok 2 Grafický priebeh zaťažujúcej sily v závislosti od teploty. Dekompozícia efektívnej hypotézy
(1) záťažová sila, (2) teplota zvárania

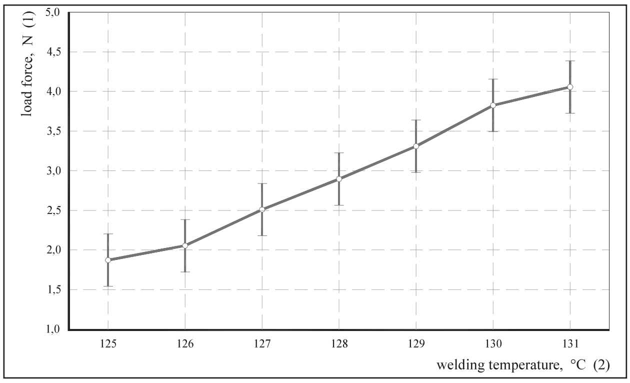

Figure 3 Graph of load force versus welding temperature. Decomposition of effective hypothesis

Obrázok 3 Grafický priebeh zaťažujúcej sily v závislosti od teploty. Dekompozícia efektívnej hypotézy

Table 1 One-way analysis of variance for the foil EK – FLEX NO 050 – 100 – FM welded with the sterile paper STERIKRAFT D

Factors of variability (1)	Sum of squares (2)	Degrees of freedom (3)	Variance (4)	F-test (5)	p-value (6)
Abs. element	841.5939	1	841.5939	4618.102	0.00
Temperature in °C	73.3221	6	12.2203	67.057	0.00
Error	19.1350	105	0.1822	–	–

Tabuľka 1 Jednofaktorová analýza fólie EK – FLEX NO 050 – 100 – FM zváranej so sterilným papierom STERIKRAFT D
(1) faktor premenlivosti, (2) suma štvorcov, (3) stupne voľnosti, (4) rozptyl, (5) F-test, (6) p-hodnota

Table 2 Basic statistical characteristics of the weld strength for the foil EK – FLEX NO 050 – 100 – FM welded with the sterile paper STERIKRAFT D

Number of measurements (1)	Temperature in °C (2)	Mean value in N.15 mm^{-1} (3)	Standard error (4)	Significance level 95 % (5)		Number of repetitions (8)
				lower (6)	upper (7)	
1	129	1.788069	0.1882	1.576456	1.999681	16
2	130	2.081113	0.2461	1.869501	2.292726	16
3	131	2.207866	0.2749	1.996253	2.419479	16
4	132	2.547741	0.3480	2.336128	2.759354	16
5	133	2.974978	0.3934	2.763365	3.186591	16
6	134	3.227041	0.5391	3.015429	3.438654	16
7	135	4.361660	0.7327	4.150048	4.573273	16

Tabuľka 2 Základné štatistické charakteristiky pevnosti zvaru fólie EK – FLEX NO 050 – 100 – FM zváranej so sterilným papierom STERIKRAFT D
(1) počet meraní, (2) teplota, (3) priemerná hodnota, (4) štandardná chyba, (5) hladina významnosti, (6) dolná, (7) horná, (8) počet opakovaní

Table 3 One-way analysis of variance for the foil ED – FLEX NO 030 – 070 – FM welded with the sterile paper STERIKRAFT D

Factors of variability (1)	Sum of squares (2)	Degrees of freedom (3)	Variance (4)	F-test (5)	p-value (6)
Abs. element	970.1734	1	970.1734	2 882.710	0.0
Temperature in °C	70.1319	6	11.6886	34.732	0.0
Error	35.3377	105	0.3365	–	–

Tabuľka 3 Jednofaktorová analýza fólie ED – FLEX NO 030 – 070 – FM zváranej so sterilným papierom STERIKRAFT D
(1) faktor premenlivosti, (2) suma štvorcov, (3) stupne voľnosti, (4) rozptyl, (5) F-test, (6) p-hodnota

Table 4 Basic statistical characteristics of the weld strength for the foil ED – FLEX NO 030 – 070 – FM welded with the sterile paper STERIKRAFT D

Number of measurements (1)	Temperature in °C (2)	Mean value in N.15 mm^{-1} (3)	Standard error (4)	Significance level 95 % (5)		Number of repetitions (8)
				lower (6)	upper (7)	
1	125	1.866754	0.1450	1.5791	2.1543	16
2	126	2.057796	0.6242	1.7702	2.3453	16
3	127	2.520229	0.3154	2.2326	2.8078	16
4	128	2.902579	0.5612	2.6150	3.1901	16
5	129	3.324867	0.4972	3.0372	3.6124	16
6	130	3.850458	0.7429	3.5628	4.1380	16
7	131	4.079521	0.9215	3.7919	4.3670	16

Tabuľka 4 Základné štatistické charakteristiky pevnosti zvaru fólie ED – FLEX NO 030 – 070 – FM zváranej so sterilným papierom STERIKRAFT D
(1) počet meraní, (2) teplota, (3) priemerná hodnota, (4) štandardná chyba, (5) hladina významnosti, (6) dolná, (7) horná, (8) počet opakovaní

mm^{-1} to 4.07 N.15 mm^{-1}. The graphical representation of weld strength versus temperature is shown in Figure 3.

Conclusions

The experimental measurements conducted in determining the weld strength enabled to find the welding temperature values optimum for packaging materials used for packaging medical products.

These results lead to the conclusion that the weld strength depends on the welding temperature and welded material. The weld strength of packaging materials in packaging disposable medical sets is important in the sterilisation process, where pouches with medical products and primarily their welds withstand high-pressure gases and there is the highest risk of breakage with a subsequent contamination and degradation of the actual content.

Laboratory results can be used as a guide for selecting an appropriate combination of the most-used materials for packaging disposable medical sets. Experimental measurements revealed the highest weld strength of 4.36 N.15 mm^{-1} at 131 °C for the combination of foil ED – FLEX NO 050 – 100 – FM welded with the sterile paper STERIKRAFT D. The results of measurements meet Standard STN EN 868-5 „Packaging materials and systems for medical devices which are to be sterilised“, where tensile strength that results in breakage of the weld must be at least 1.5 N.15 mm^{-1}.

Súhrn

Cieľom práce bolo stanoviť pevnosť zvaru skúmaných obalových materiálov, ktoré sa používajú pri balení zdravotníckych výrobkov. Preplátované spoje obalových materiálov boli zvárané diskontinuálnym nepriamym zváracím zariadením pri tlaku 0,5 MPa. Na výsledok pevnosti zvaru vplýva teplota zváracieho materiálu, doba zvárania a tlak zváracích čeľustí. Z vyhodnotených meraní najlepšiu pevnosť zvaru sme zistili pri zváraní obalového materiálu ED – FLEX NO 058 – 100 – FM so sterilným papierom STERIKRAFT D.

Kľúčové slová: pevnosť zvaru, teplota zvárania, trhací stroj

References

ČURDA, D. 2001. Vlastnosti obalu pro balení potravin. In: Svět balení, 2001, č. 2, s. 10 – 12. ISSN 1212-7809.

LUKÁŠ, J. 1990. Navrhování a konstrukce obalů 1. Praha : SPN, 1990, 235 s. ISBN 80-04-23415-1.

MARTINEC, Ľ. – PAŠEK, J. – KÓNICKÁ, V. 1991. Zváranie plastických látok Z-U9. Bratislava : Dom techniky, 1991. 124 s. ISBN 80-233-0218-3.

MARTINEC, Ľ. – PINKAVOVÁ, Ľ. 1989. Možnosti stanovenia teplom ovplyvnenej oblasti zváraných spojov polyolefínov. In: Plasty a jejich zkoušení. Brno : DT ČSVTS, 1989, s. 84 – 88. ISBN 80-02-99577-0.

NEMCOVÁ, A. – KHANDL, F. 1996. Spájanie plastov. Bratislava : Weldtech, 1996. 38 s. ISBN 80-88734-18-5.

ŠTAUDNER, E. 1984. Fyzikálne metódy skúmania plastických látok. Bratislava : ES SVŠT, 1984. 188 s.

VALŠÍKOVÁ, M. – KOPEC, K. 2009. Pozberová technológia záhradníckych plodín. Nitra : SPU. 2009, 158 s. ISBN 978-80-552-0313-3.

ZEMAN, S. 2008. Balenie a obalová technika. Nitra : SPU. 2005, 188 s. ISBN 978-80-552-0117-7.

STN 77 0140:1990. Obalové materiály. Zásady zvárania a stanovenia pevnosti zvaru.

STN EN 868-5:2001. Obalové materiály a systémy balenia zdravotníckych prístrojov určených na sterilizáciu. Časť 5: Teplom uzavierateľné a samolepiace priesvitné vrecia a rúrky z papiera a plastových fólií. Požiadavky a skúšobné metódy.

Contact address:
doc. Ing. Stanislav Zeman, PhD., Ing. Martin Pršan, PhD., Faculty of Engineering, Department of Production Engineering, Slovak University of Agriculture in Nitra, Tr. A. Hlinku 2, 949 76 Nitra, Slovak Republic, tel.: +421 37 641 4300, fax: +421 37 74 17 003, e-mail: Stanislav.Zeman@uniag.sk, prof. Ing. Magdaléna Valšíková, PhD., Horticulture and Landscape Engineering Faculty, Department of Vegetables Production, Slovak University of Agriculture in Nitra, tel. +421 37 641 4226, e-mail: Magdalena.Valsikova@uniag.sk